



## Research paper

# Inclusion of a 5-fluorouracil moiety in nitrogenous bases derivatives as human carbonic anhydrase IX and XII inhibitors produced a targeted action against MDA-MB-231 and T47D breast cancer cells

Andrea Petreni<sup>a</sup>, Alessandro Bonardi<sup>a</sup>, Carrie Lomelino<sup>b</sup>, Sameh M. Osman<sup>c</sup>, Zeid A. ALOthman<sup>c</sup>, Wagdy M. Eldehna<sup>d</sup>, Radwan El-Haggar<sup>e</sup>, Robert McKenna<sup>b</sup>, Alessio Nocentini<sup>a,\*</sup>, Claudiu T. Supuran<sup>a,\*\*</sup>

<sup>a</sup> University of Florence, Department of NEUROFARBA, Section of Pharmaceutical and Nutraceutical Sciences, via Ugo Schiff 6, 50019, Sesto Fiorentino, Florence, Italy

<sup>b</sup> University of Florida, Department of Biochemistry and Molecular Biology, 1200 Newell Dr, Gainesville, FL, 32610, USA

<sup>c</sup> Chemistry Department, College of Science, King Saud University, P. O. Box 2455, Riyadh, 11451, Saudi Arabia

<sup>d</sup> Department of Pharmaceutical Chemistry, Faculty of Pharmacy, Kafrelsheikh University, Kafrelsheikh, 33516, Egypt

<sup>e</sup> Pharmaceutical Chemistry, Department, Faculty of Pharmacy, Helwan University, 11795, Cairo, Egypt

## ARTICLE INFO

## Article history:

Received 15 January 2020

Received in revised form

31 January 2020

Accepted 31 January 2020

Available online 3 February 2020

## Keywords:

Anticancer

5-Fluorouracil

Carbonic anhydrase

Selectivity

Annexin

Breast cancer

## ABSTRACT

A new series of pyrimidine derivatives as human carbonic anhydrases (CA, EC 4.2.1.1) inhibitors is here designed by including a 5-fluorouracil (5-FU) moiety, broadly used anticancer medication, in nitrogenous base modulators of the tumor-associated CAs. Most sulfonamide derivatives efficiently inhibit the target CA IX ( $K_s$  in the range 0.47–44.7 nM) and CA XII ( $K_s$  in the range 2.9–83.1 nM), while the 5-FU coumarin derivatives showed a potent and totally selective inhibitory action against the target CA IX/XII over off-target CA I/II. The X-ray solved crystal structure of CA II in adduct with a representative uracil derivative provided insights on the binding mode to the target of such pyrimidine derivatives. On the basis of potency and selectivity inhibition profiles, coumarin **12a**, the sulfonamide CAs showing the greatest II/IX specificity (**4e**, **6b** and **6d**) and the unique subnanomolar CA IX inhibitor **10a** were tested *in vitro* for their antiproliferative action against a panel of eight cancer cell lines. The breast cancer cell lines MDA-MB-231 and T47D were the most susceptible with  $IC_{50}$  values in low to medium micromolar ranges ( $2.45 \pm 0.07$ – $18.86 \pm 0.72$   $\mu$ M and  $6.86 \pm 0.31$ – $40.92 \pm 1.59$   $\mu$ M, respectively). A cell cycle analysis showed that **4e** and **6d** arrest T-47D cells mainly in the G2/M phase. Using an annexin V-FITC apoptosis assay, **4e** and **6d** were shown to induce an approximately 23.6-fold and 34.8-fold total increase in apoptosis compared to the control, corroborating the concrete potential of 5-FU CAs for the design of new effective anticancer strategies.

© 2020 Elsevier Masson SAS. All rights reserved.

## 1. Introduction

Hypoxic induced cancer cells adapt their metabolism via a glycolytic shift, which decreases extracellular pH and modifies their genes expression pattern to survive in an environment incompatible for normal cell growth [1,2]. Among the membrane proteins overexpressed by hypoxic tumors to regulate

pH are the carbonic anhydrases (CA, EC 4.2.1.1) [3], that catalyze the reversible hydration of carbon dioxide to bicarbonate ion and a proton. In this context, the transmembrane isoforms CA IX and XII participate in the pH regulation of the extracellular environment [3–5]. CA IX is not appreciably expressed in most normal tissues, while its up-regulation is associated with hypoxic cancer phenotypes, where it is strongly induced via the hypoxia inducible factor-1 $\alpha$  (HIF-1 $\alpha$ ) [6–8]. CA XII is also implicated in the extracellular acidification in many tumor types [4,9]. As a result, CA IX and XII are factors driving tumor growth, invasiveness, proliferation, metastasis, as well as resistance to radio- and chemotherapy [10]. This makes agents

\* Corresponding author.

\*\* Corresponding author.

E-mail addresses: [alessio.nocentini@unifi.it](mailto:alessio.nocentini@unifi.it) (A. Nocentini), [claudiu.supuran@unifi.it](mailto:claudiu.supuran@unifi.it) (C.T. Supuran).

inhibiting CA IX and XII, in a selective manner, a valuable therapeutic for the targeting of the primary tumor growth, invasion metastasis, and the reduction of cancer stem cell population [10–12].

The issue with sulfonamide-like CA inhibitors (CAIs), the main inhibitory chemotypes adopted for therapeutic purposes, is a promiscuous action against almost all isoforms encoded in humans, that results in non-selective targeting, and therefore undesired side effects [6]. In fact, the comparison of the 12 catalytically active human CAs demonstrates a high sequence homology within the active sites that increases the difficulties in the design of disease-targeted inhibitors [13]. Among the strategies adopted to bypass this issue are the optimization of CAIs (i.e. the tail approach [12], whose application produced **SLC-0111** [14], the first-in-class CAI entering clinical trials for the treatment of hypoxic tumors) or the use of alternative chemotypes, such as coumarin and bioisosters which use different chemotypes for enzymatic inhibition [4,11].

As an application of the tail approach, we recently reported two series of uracil/adenine-tailed benzenesulfonamides as potent CA IX inhibitors (series 1 and 2, Fig. 1) [15]. Purine/pyrimidine-based scaffolds are considered privileged structures in the drug-design of bioactive compounds because of synthetic accessibility and ability to confer drug-like properties [16,17]. In particular, pyrimidines and purines are widely used as antitumor and antiviral pharmacophores in medicinal chemistry, due their ability to interfere with the DNA functions in diverse manners [18,19]. A selection of the reported CAIs showed significant anti-proliferative activity against HT-29 colon cancer cell lines [15].

As a continuation of the previous work, the uracil derivatives series is here developed by swapping the nitrogenous base to a 5-fluorouracil (5-FU), a clinically used chemotherapeutic agent, to produce series 3 (Fig. 1). A major number of benzenesulfonamide scaffolds as CAIs was investigated as well as coumarin cores to achieve a more targeted CA IX/XII inhibition. A subset of 5-FU CAIs was evaluated *in vitro* against eight cancer cell lines. The effects of the two more active compounds on the phases of cell cycle and annexin V-FITC-positive staining in breast T47D cells were thereafter assessed.

## 2. Results and discussion

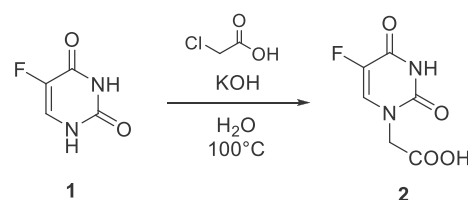
### 2.1. Drug design and chemistry

5-FU is widely used medication in the treatment of cancer [20]. Over the past 20 years, increased understanding of the mechanism of action of 5-FU, principally based on the inhibition of thymidylate synthase, has led to the development of strategies that increase its anticancer activity.

A molecular hybridization approach is here adopted combining 5-FU with CAI scaffolds to synergize the inhibition of the tumor-associated isozymes with intrinsic anticancer effects resulting by the pyrimidine pharmacophore [21].

5-FU was incorporated through the N1 atom on a wealth of benzenesulfonamide structures by amide or triazole linkers to explore the chemical space within the target and off-target CAs binding sites. A small subset of ester, amide or triazole linked 5-FU coumarin derivatives was also produced to yield markedly selective CA IX/XII 5-FU-based inhibitors. In fact, coumarins act as prodrug which undergo a CA mediated hydrolysis and the formed species (*E*- or *Z*-cinnamic acid) accomplishes the enzymatic inhibition by occluding the entrance of the active site [11,12]. The latter is the most variable region, in terms of amino acid residues, among the human CAs. The cancer-related CAs were shown to be more prone to such a kind of inhibition mechanism than ubiquitous CAs.

Intermediate **2** was provided by reacting 5-FU with chloroacetic acid in KOH<sub>(aq)</sub> (Scheme 1). The carboxylic acid **2** was thus coupled with a variety of primary (**3a-e**) and secondary (**5a-f**) amine benzenesulfonamide derivatives using 1-ethyl-3-(3-



Scheme 1. Synthesis of intermediate **2**.

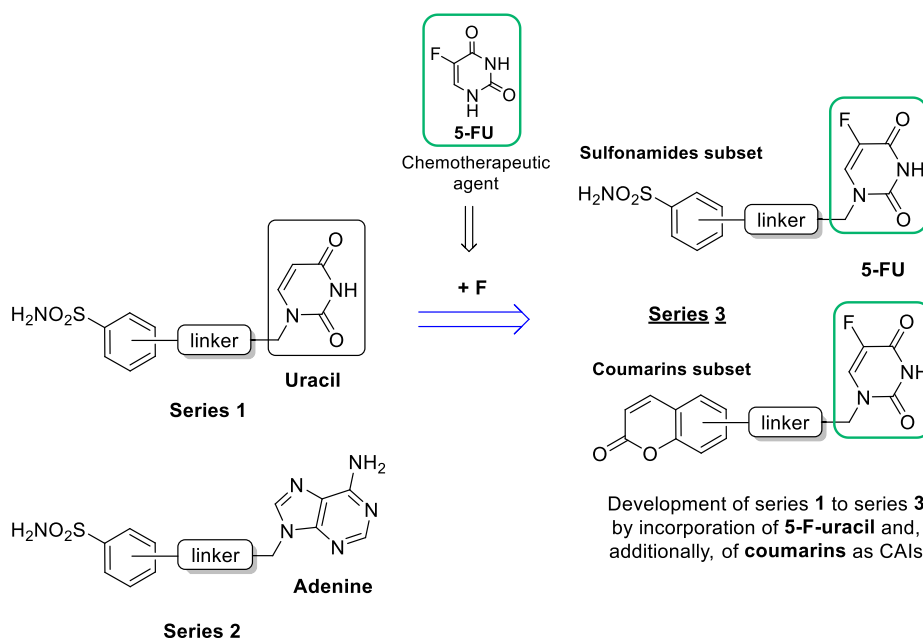
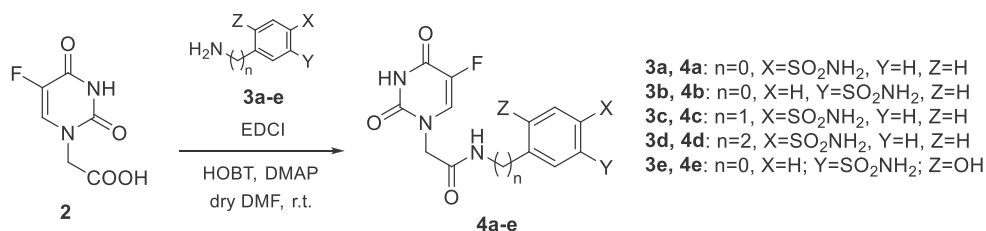
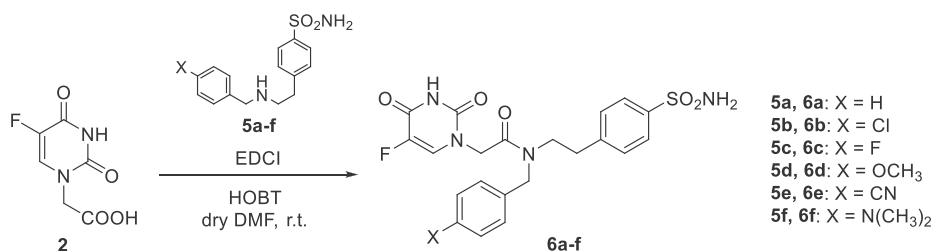
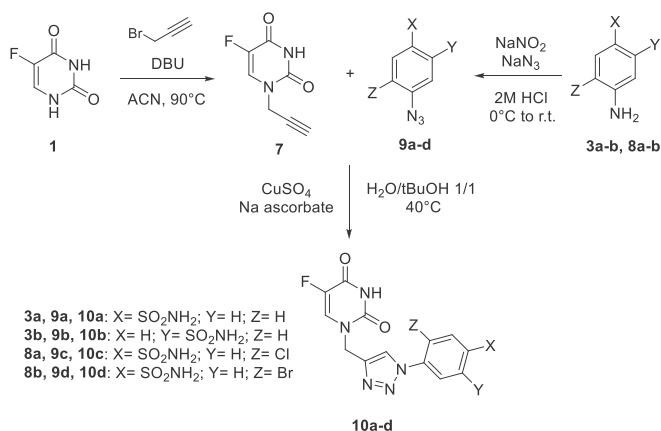
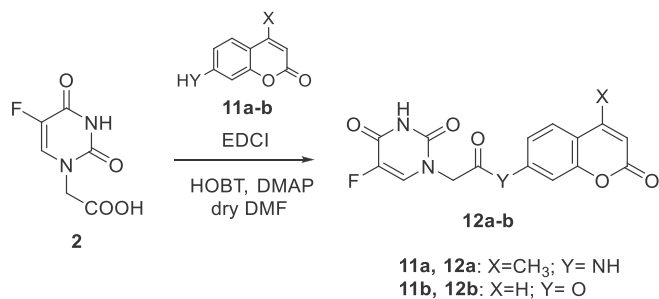


Fig. 1. Drug-design of 5-fluorouracil derivatives as antitumor CAIs.

Scheme 2. Synthesis of amides **4a-4e**.Scheme 3. Synthesis of amides **6a-6f**.Scheme 4. Synthesis of triazoles **10a-d**.Scheme 5. Synthesis of coumarins **12a-b**.

dimethylaminopropyl)carbodiimide (EDC) in presence of 1-hydroxybenzotriazole (HOBT) and 4-dimethylaminopyridine (DMAP) to yield amides **4a-e** (Scheme 2) and **6a-f** (Scheme 3) [15].

The triazole derivatives (**10a-d**) were generated by a Cu(I) catalyzed azide-alkyne cycloaddition (CuAAC) between the N1-propargyluracil **7** and the freshly prepared azides **9a-d** yielded by a Sand-Meyer reaction (Scheme 4).  $\text{CuSO}_4$  and vitamin C were used

to generate *in situ* the Cu(I) catalyst.

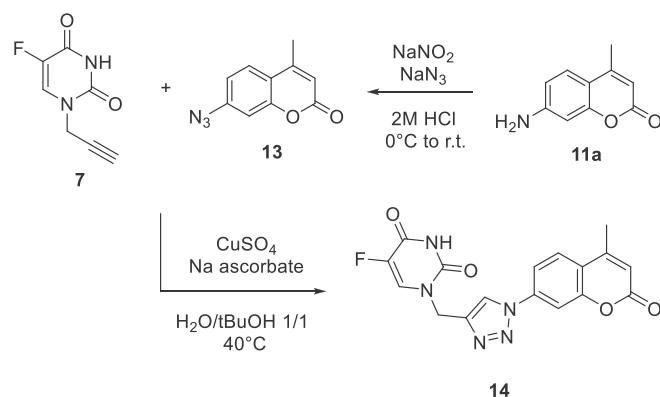
The coumarin derivatives **12a** and **12b** were prepared by coupling intermediate **2** with 7-amino-4-methylcoumarin **11a** and umbelliferone **11b**, respectively, adopting again EDC as coupling agent (Scheme 5). The CuAAC between alkyne **7** and coumarin azide **13** yielded triazole **14** (Scheme 6).

Compounds **4a-e**, **6a-f**, **10a-d**, **12a-b**, **14** were obtained in high yields and thoroughly characterized by  $^1\text{H}$ -,  $^{13}\text{C}$ -,  $^{19}\text{F}$  NMR and HRMS.

## 2.2. Carbonic anhydrases inhibition

The CA inhibitory action of 5-FU compounds **4a-e**, **6a-f**, **10a-d**, **12a-b**, **14**, was assessed against the cytosolic CA I and II (ubiquitous) and CA IX and XII (cancer-related) isoforms by a stopped flow  $\text{CO}_2$  hydrase assay, in addition to acetazolamide (AAZ) as standard inhibitor [22]. The following structure-activity relationship (SAR) can be drawn up from the inhibition data reported in Table 1.

The cytosolic off-target CA I was the least inhibited isoform. The inhibition constants ( $K_i$ s) of the sulfonamide 5-FU derivatives spanned between 207.6 and 9679.8 nM. The *m*-substitution at the benzenesulfonamide scaffold produced the least CA I inhibition, such as in compounds **4b** ( $K_i$  of 5.1  $\mu\text{M}$ ), **4e** ( $K_i$  of 9.7  $\mu\text{M}$ ) and **10b** ( $K_i$  of 8.9  $\mu\text{M}$ ). Additionally, the *p*-chloro substituted secondary amide **6b** inhibited CA I by a micromolar value ( $K_i$  of 2.6  $\mu\text{M}$ ). The removal

Scheme 6. Synthesis of coumarin **14**.

**Table 1**  
Inhibition data of human CA isoforms I, II, IX and XII with 5-FU derivatives **4a-e**, **6a-f**, **10a-d**, **12a-b**, **14** and the standard acetazolamide (**AAZ**) by a stopped flow CO<sub>2</sub> hydrase assay [22]. Compounds selected for *in vitro* anticancer assays are highlighted in gray.

Cmpd	K <sub>i</sub> (nM) <sup>a</sup>			
	CA I	CA II	CA IX	CA XII
<b>4a</b>	323.5	6.8	4.8	4.7
<b>4b</b>	5158.3	81.5	44.7	66.3
<b>4c</b>	738.6	101.3	29.2	40.1
<b>4d</b>	299.3	19.6	24.8	7.0
<b>4e</b>	9679.8	9083.9	452.8	59.5
<b>6a</b>	207.6	0.59	3.5	2.9
<b>6b</b>	2965.0	34.8	4.2	6.2
<b>6c</b>	933.9	13.4	11.8	4.8
<b>6d</b>	727.4	8.0	1.9	9.0
<b>6e</b>	383.6	0.71	4.9	28.6
<b>6f</b>	581.9	5.1	26.8	15.5
<b>10a</b>	651.0	0.67	0.47	9.8
<b>10b</b>	8911.2	89.2	105.3	83.1
<b>10c</b>	656.1	2.4	11.2	8.4
<b>10d</b>	626.3	0.81	3.8	3.9
<b>12a<sup>b</sup></b>	>10,000	>10,000	16.5	23.2
<b>12b<sup>b</sup></b>	>10,000	>10,000	36.8	14.4
<b>14<sup>b</sup></b>	>10,000	>10,000	173.4	408.4
<b>AAZ</b>	250.0	12.5	25.0	5.7

<sup>a</sup> Mean from 3 different assays, by a stopped flow technique (errors were in the range of  $\pm 5$ –10% of the reported values).

<sup>b</sup> Incubation time of 6h

of the chlorine atom in the latter compound led instead to best CA I inhibitor that is **6a** (K<sub>i</sub> of 207.6 nM). The elongation of the spacer between the benzenesulfonamide and the primary amide moiety reduced the CA I inhibitory activity passing from 0 (**4a**) to 1 (**4c**) carbon atom, while it is restored to a 300 nM value approximately when a second carbon atom unit was introduced (**4d**).

The most physiologically relevant isoform CA II was effectively inhibited by most 5-FU based sulfonamide derivatives. In fact, K<sub>i</sub>s spanned in the range 0.59–34.8 nM, except for **4b** (K<sub>i</sub> of 81.5 nM), **4c** (K<sub>i</sub> of 101.3 nM) and **10b** (K<sub>i</sub> of 89.2 nM), while **4e** barely inhibited CA II below 10  $\mu$ M (K<sub>i</sub> of 9.1  $\mu$ M). Again, *m*-substitutions at the benzenesulfonamide core was detrimental for CA inhibition with respect to *p*-substitutions, as well as a 1-carbon atom linker between zinc-binding portion and amide linker (**4c**). A subset of

**Table 2**  
Selectivity index (SI) calculated for human CA IX and XII over off-targets isoforms as ratio between K<sub>i</sub>s.

Cmpd	Selectivity Index (SI)			
	I/IX	II/IX	I/XII	II/XII
<b>4a</b>	67.4	1.4	68.8	1.4
<b>4b</b>	115.4	1.8	77.8	1.2
<b>4c</b>	25.3	3.5	18.4	2.5
<b>4d</b>	12.1	0.8	42.8	2.8
<b>4e</b>	21.4	20.1	162.7	152.7
<b>6a</b>	59.3	0.2	71.6	0.2
<b>6b</b>	706.0	8.3	478.2	5.6
<b>6c</b>	79.1	1.1	194.6	2.8
<b>6d</b>	382.8	4.2	80.8	0.9
<b>6e</b>	78.3	0.1	13.4	<0.1
<b>6f</b>	21.7	0.2	37.5	0.3
<b>10a</b>	1385.1	1.4	66.4	0.1
<b>10b</b>	84.6	0.8	107.2	1.1
<b>10c</b>	58.6	0.2	78.1	0.3
<b>10d</b>	164.8	0.2	160.6	0.2
<b>12a</b>	>606.1	>606.1	>431.0	>431.0
<b>12b</b>	>271.7	>271.7	>694.4	>694.4
<b>14</b>	>57.7	>57.7	>24.5	>24.5
<b>AAZ</b>	10.0	0.5	43.9	2.2

**Table 3**  
K<sub>i</sub> ratio between 5-FU derivatives and corresponding non-fluorinated compounds from series A (uracil derivatives) when applicable.

Cmpd	K <sub>i</sub> uracil derivative (series A)/K <sub>i</sub> 5-FU derivative (series C)		
	CA I	CA II	CA IX
<b>4a</b>	2.0	2.6	5.3
<b>4b</b>	1.5	8.6	69.8
<b>4c</b>	2.1	4.9	13.9
<b>4d</b>	2.2	2.1	1.8
<b>4e</b>	1.0	0.5	1.0
<b>10a</b>	0.4	1.4	10.2
<b>10b</b>	0.5	4.3	4.4

derivatives inhibited CA II in a subnanomolar range, that are the unsubstituted and *p*-CN benzyl amide compounds **6a** (K<sub>i</sub> of 0.59 nM) and **6e** (K<sub>i</sub> of 0.71 nM) and the *p*-triazole benzenesulfonamide derivatives **10a** (K<sub>i</sub> of 0.71 nM) and **10d**, that is also substituted in *meta* by a bromine atom (K<sub>i</sub> of 0.81 nM). Swapping the *p*-CN group with a chlorine atom (**6b**), a fluorine atom (**6c**), a methoxy group (**6d**) and a dimethylamino group (**6e**) reduced the CA inhibitory action by 7 to 50-fold.

The main antitumor target CA IX was also efficiently inhibited by most 5-FU sulfonamide derivatives with K<sub>i</sub>s ranging between 0.47 and 44.7 nM. Uniquely, the *m*-substituted **4e** and **10b** induced inhibition above 100 nM, with K<sub>i</sub>s of 452.8 and 105.3, respectively. A single subnanomolar CA inhibitor was identified against CA IX, that is the triazole **10a**, whose K<sub>i</sub> of 0.47 nM represents the best CA inhibition here reported. Among the *N*-benzyl substituted secondary amides **6a-f**, the *p*-OCH<sub>3</sub> derivative **6d** stood out as the most active one with a K<sub>i</sub> of 1.9 nM. Notably, a significant subset of 5-FU CAIs inhibit CA IX more capably than the clinically used **AAZ** (K<sub>i</sub> of 25.0 nM).

CA XII, the second tumor-related CA, was inhibited by most sulfonamide CAIs reported here with an overall comparable range with CA II and IX, though with diverse SAR. K<sub>i</sub>s spanned in the range 2.9–83.1 nM and no subnanomolar inhibition was detected. The worst K<sub>i</sub>s, detected in the range 59.5–83.1 nM, are consistently associated with the *m*-substituted **4b**, **4e** and **10b**. The introduction of a 1-carbon atom linker between zinc-binding portion and amide linker (**4c**) decreased CA IX inhibition below the average as well (K<sub>i</sub> of 40.1 nM). The *N*-benzyl substituted secondary amides showed a rather flat inhibitory trend with K<sub>i</sub>s spanning in the range

**Table 4**  
X-ray crystallography statistics for structure of CA II in complex with compound **A**.

CA II - A	
<b>PDB Accession Code</b>	6VJ3
<b>Space Group</b>	P2 <sub>1</sub>
<b>Cell Dimensions (Å; °)</b>	$a = 42.5, b = 41.4, c = 72.2;$ $\beta = 104.4$
<b>Resolution (Å)</b>	32.2–1.4 (1.40–1.35)
<b>Total Reflections</b>	164,794
<b>I/σ</b>	12.9 (1.5)
<b>Redundancy</b>	3.1 (2.1)
<b>Completeness (%)</b>	98.0 (88.0)
<b>Rcryst (%)</b>	15.1 (27.2)
<b>Rfree (%)</b>	15.2 (28.4)
<b># of Protein Atoms</b>	2069
<b># of Ligand Atoms</b>	51
<b>Ramachandran stats (%):</b>	97.3, 2.7, 0.0
<b>  favored, allowed,</b>	
<b>  generously allowed</b>	
<b>Avg. B factors (Å<sup>2</sup>): Main-chain,</b>	15.8, 23.8, 25.7
<b>  Ligand, Solvent</b>	
<b>rmsd for bonds, angles (Å, °)</b>	0.007, 1.12

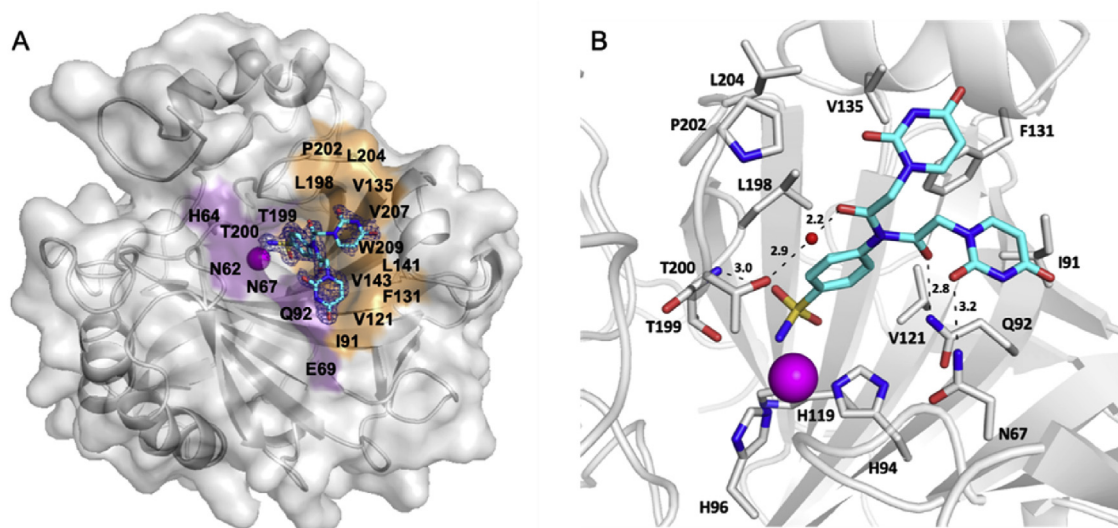


**Fig. 2.** A) Surface representation of CA II in complex with compound **A** from series 1, the uracil (F-devoid) analog of compound **4a** (shown as cyan sticks). Hydrophobic and hydrophilic residues of the active site are labeled and colored orange and purple, respectively. B) Active site view of compound **A** binding. Hydrogen bonds are shown as black dashes with distances labeled in Å. (For interpretation of the references to color in this figure legend, the reader is referred to the Web version of this article.)

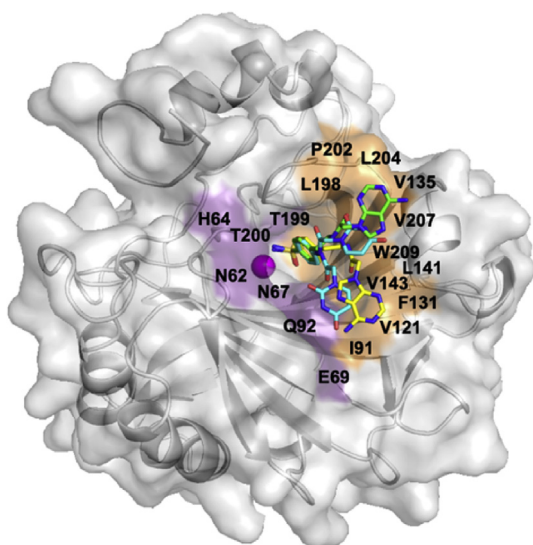


**Fig. 3.** Overlay of compound **A** (cyan sticks) and compound **B**, an adenine derivative (adenine analog of **4d**) from series 2 (green sticks in CA II and yellow sticks in CA IX-mimic binding) in surface representation of CA II. (For interpretation of the references to color in this figure legend, the reader is referred to the Web version of this article.)

2.9–28.6 nM. The best value is associated to the unsubstituted **6a** while the worst value is related to the *p*-CN substitution of **6e**. Among the triazole derivatives **10a–d** the introduction of *m*-Br substituent on the benzenesulfonamide scaffold produced the best CA XII inhibition ( $K_i$  of 3.9 nM).

In contrast, the 5-FU coumarin derivatives **12a–b** and **14** showed a potent and totally selective inhibitory action against the target CA IX/XII over CA I/II. In detail, the three compounds did not inhibit CA I and II, lower than 10  $\mu$ M. Whereas, CA IX and XII were inhibited in similar ranges, 16.5–173.4 nM and 14.4–408.4 nM, respectively. However, while amide **12a** was the best CA IX inhibitor ( $K_i$  of 16.5 nM), CA XII turned out to be slightly more efficiently inhibited by ester **12b**. The triazole coumarin **14** exhibited a decrease of efficacy against both cancer-related CAs.

As for target/off-target CAs selectivity ratio of action of sulfonamide 5-FU derivatives, all compounds exhibited remarkable I/IX and I/XII inhibitory specificity, as the calculated selectivity index (*SI*) spans in the ranges 12.1–1385.1 and 13.4–478.2, respectively (Table 2). In contrast, only two distinct subsets of sulfonamide derivatives (approximately half of the compounds) produced a preferred inhibition of the target CA IX and XII over the main off-target CA II. In detail, only the 1-carbon atom spacer derivative **4c**, the *m*-substituted **4e** and the N-benzyl amides **6b** and **6d** reported significant II/IX *SI* spanning between 3.5 and 20, that are greater than that measured for the standard **AAZ**. As for II/XII *SI* values, oddly the 1- and 2-carbon atoms spacer derivative **4c** and **4d**, the *m*-substituted **4e** and the N-benzyl amides **6b** and **6c** solely had values above 2, with that of **4e** even reaching the value of 153.

On the basis of the data of Table 1 and 2, coumarin **12a**, the sulfonamide CAs showing the greatest II/IX *SI*, namely **4e**, **6b** and **6d**, and the unique subnanomolar CA IX inhibitor **10a** were chosen for assessing *in vitro* their antiproliferative action against a panel of cancer cell lines.

The corresponding nonfluorinated analog (uracil derivative, from series A) was previously reported and characterized for a subset of 5-FU derivatives, namely **4a–e**, **10a–b**, and tested as inhibitor of CA I, II and IX [15]. Table 3 shows the  $K_i$  ratio against CA I, II and IX between each uracil derivative and its corresponding 5-FU analog. A significant enhancement in the CA inhibitory action was detected for most 5-FU compounds against CA II (ratio of 0.5–8.6) and CA IX (ratio of 1.0–69.8) compared to the uracil correspondents. As in most cases the increase was more intense against the target CA IX over CA II, it can be speculated that the incorporation of a fluorine atom in position 5 of the nitrogenous base scaffold increases both potency and selectivity against the target CA IX.

### 2.3. X-ray Crystallography

X-ray crystallography was utilized to observe the binding to CA II of a representative compound from the pyrimidine series, compound **A** from series 1, the uracil (F-devoid) analog of compound **4a** from series 3. This structure was determined to a resolution of 1.4 Å (Table 4). As expected for a sulfonamide-based compound, the zinc-binding group (ZBG) displaced the active site zinc-bound water

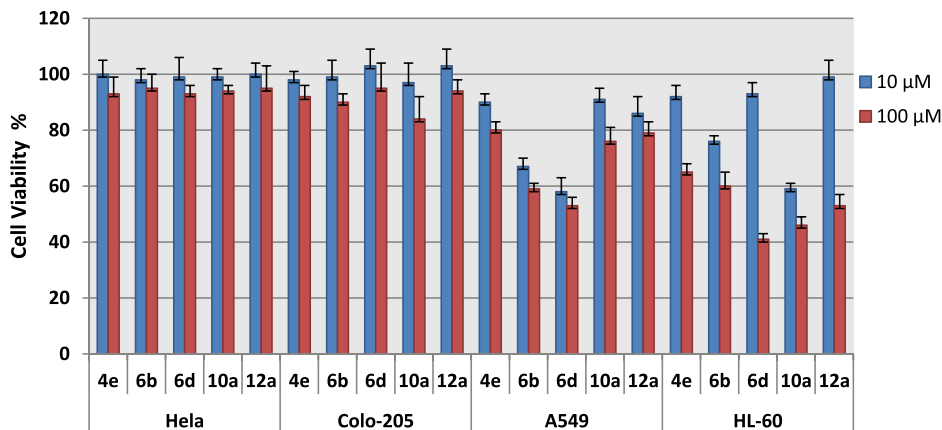


Fig. 4. Anti-proliferative activity (cell growth inhibitory activity at 10 and 100  $\mu\text{M}$  concentrations) of compounds **4e**, **6b**, **6d**, **10a** and **12a** against HeLa, Colo-205, A549 and HL-60 cancer cell lines.

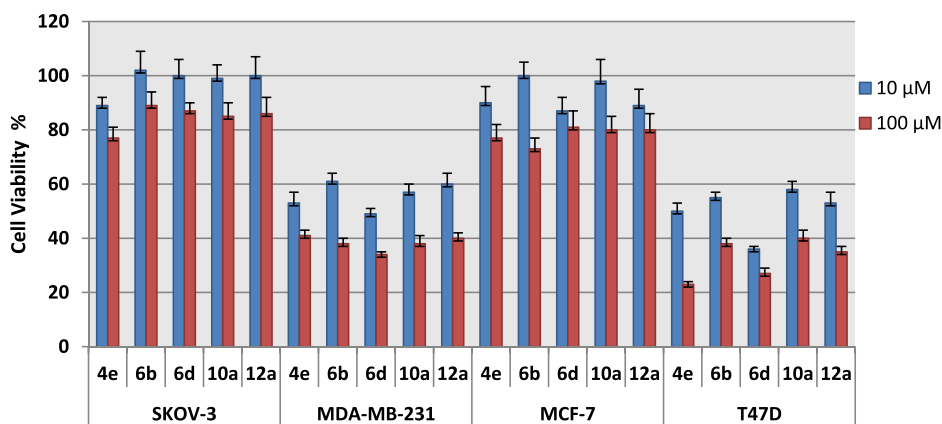


Fig. 5. Anti-proliferative activity (cell growth inhibitory activity at 10 and 100  $\mu\text{M}$  concentrations) of compounds **4e**, **6b**, **6d**, **10a** and **12a** toward SKOV-3, MDA-MB-231, MCF-7 and T47D cancer cell lines.

(ZBW) and bound directly to the zinc. The ZBG also formed a hydrogen bond between the sulfonamide oxygen and backbone amide of T199 (3.0 Å). The tail component of compound **A** was observed to exhibit dual conformations, attributed to the freedom of rotation about the amide linker, resulting in one conformation oriented towards the hydrophobic side and another extending towards the hydrophilic side of the active site (Fig. 2A). The minor tail conformation, oriented towards the hydrophobic pocket, exhibited a lower occupancy (43%) as indicated by the weaker electron density (Fig. 2A). In the minor conformer, the carbonyl of the linker forms a hydrogen bond with a water that bridges to the side chain of T199 (2.2 and 2.9 Å, respectively; Fig. 2B). In the major tail conformation, occupancy (55%), a hydrogen bond is formed between the linker carbonyl and side chain of Q92 (2.8 Å) in addition to the uracil moiety and side chain of N67 (3.2 Å) (Fig. 2B). The additional hydrogen bonding is thought to stabilize the compound tail, resulting in the observed higher occupancy. Both conformations are further stabilized by interactions with active site residues F131, V135, L198, P202, L204 and F131, I91, V121 (Fig. 2B).

Interestingly, the two orientations of compound **A** are reminiscent of the dual binding modes of a previously studied purine-based inhibitor, compound **B** from series 2, namely the adenine analog of **4d** from series 3. Compound **B** exhibited unique binding modes based on the CA isoform with the inhibitor tail orienting in the hydrophobic side in the active site of CA II and extending toward the hydrophilic side of the active site of CA IX-mimic. Despite

a shift of the linker and tail portion of compound **A** by approximately 2–3 Å due to the steric hindrance of F131, these two binding modes of compound **B** are oriented similarly to the two observed conformations of compound **A** in CA II (Fig. 3).

#### 2.4. *In vitro* anti-proliferative activity

Sulfonamides **4e**, **6b**, **6d**, **10a** and coumarin **12a** displayed efficient and/or selective inhibitory actions against the tumor-related isoforms CA IX and XII over the cytosolic off-target CA I and II (Tables 1 and 2). Accordingly, the five compounds were selected to be evaluated *in vitro* for their potential anti-proliferative activity, utilizing Sulforhodamine B colorimetric assay (SRB) as described by

Table 5

IC<sub>50</sub> of anti-proliferative activity of compounds **4e**, **6b**, **6d**, **10a** and **12a** against breast MDA-MB-231 and T47D cancer cell lines in normoxia.

Cmpd	IC <sub>50</sub> ( $\mu\text{M}$ ) <sup>a</sup>	
	MDA-MB-231	T47D
<b>4e</b>	25.46 ± 1.38	7.56 ± 0.29
<b>6b</b>	40.92 ± 1.59	18.86 ± 0.72
<b>6d</b>	6.86 ± 0.31	2.45 ± 0.07
<b>10a</b>	22.85 ± 0.91	33.51 ± 1.24
<b>12a</b>	32.04 ± 1.84	13.16 ± 0.71
<b>Staurosporine</b>	4.25 ± 0.16	4.52 ± 0.19

<sup>a</sup> IC<sub>50</sub> values are the mean ± S.D. of three separate experiments.

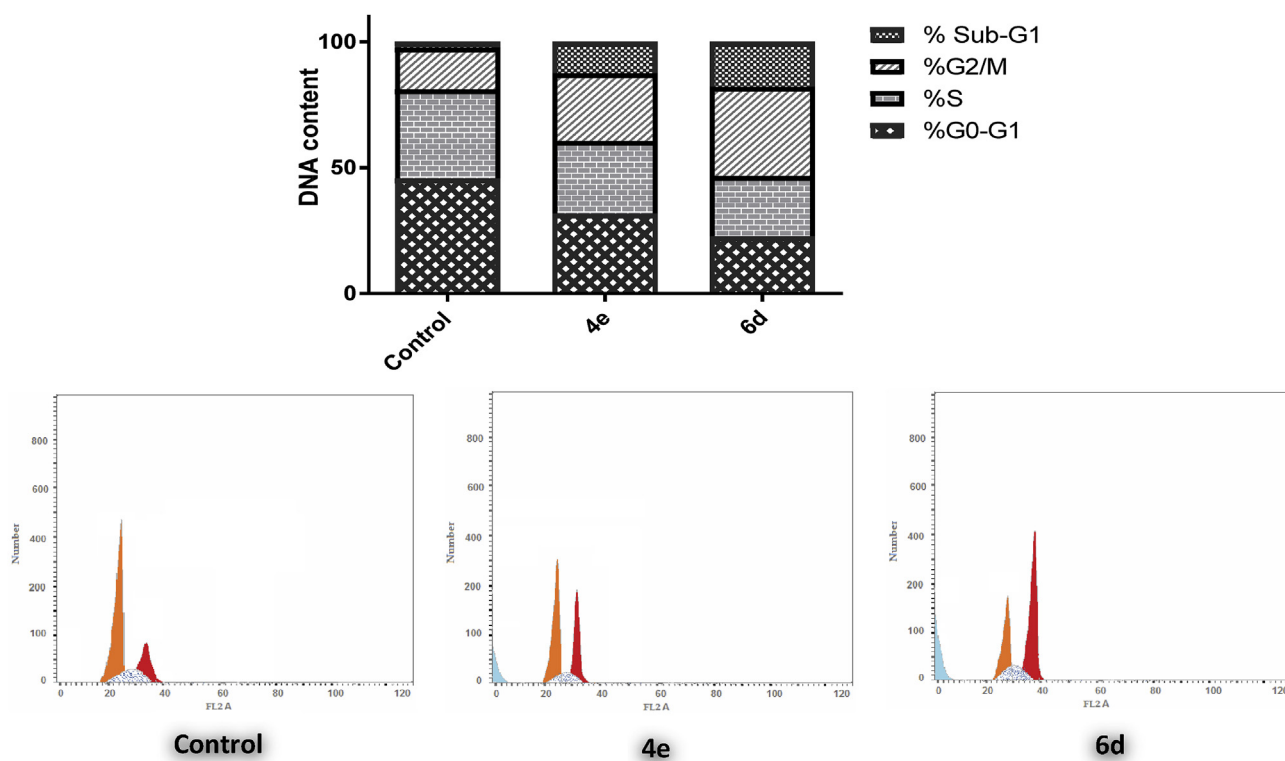


Fig. 6. Effect of sulfonamides **4e** and **6d** on the phases of cell cycle of T47D cells.

Skehan et al.

The anti-proliferative activities of **4e**, **6b**, **6d**, **10a** and **12a** were first evaluated in a preliminary screening against eight cancer cell lines, namely cervical (Hela), colon (Colo-205), lung (A-549), leukemia (HL-60), ovarian (SKOV-3), and breast (MDA-MB-231, MCF-7 and T47D) cancer cell lines. This initial assessment of antitumor activity tested each derivative in triplicate at 10 and 100  $\mu\text{M}$  concentrations, and the data were presented as percentage cell viability caused by each tested compound (Figs. 4 and 5).

The tested derivatives showed different levels of growth inhibitory activity and possessed a distinctive pattern of selectivity toward the examined eight cancer cell lines. Close examination of the cell viability % in Figs. 4 and 5 hinted out that breast cancer MDA-MB-231 and T47D cells were the most susceptible examined cell lines to the influence of the tested compounds, with cell viability % range of (49–61 and 36–58, respectively) at 10  $\mu\text{M}$  and (34–41 and 49–61, respectively) at 100  $\mu\text{M}$  (Fig. 5). Moreover, lung A-549 and leukemia HL-60 cells were moderately affected by the tested compounds, with cell viability % range of (58–91 and 59–99, respectively) at 10  $\mu\text{M}$  and (53–80 and 41–65, respectively) at 100  $\mu\text{M}$  (Fig. 4), whereas, the tested compounds (**4e**, **6b**, **6d**, **10a** and **12a**) displayed weak or no growth inhibitory activities towards cervical Hela, colon Colo-205, ovarian SKOV-3, and breast MCF-7 cancer cell lines.

Therefore, the quantitative  $\text{IC}_{50}$  values were determined for sulfonamides **4e**, **6b**, **6d** and **10a** and coumarin **12a** against the most susceptible cancer cell lines in the preliminary screening (MDA-MB-231 and T47D), testing concentrations of 100, 10, 1, 0.1 and 0.01  $\mu\text{M}$  for 72h (Table 5).

As indicated in Table 5, the tested compounds were more effective against T47D ( $\text{IC}_{50}$  range:  $2.45 \pm 0.07$ – $18.86 \pm 0.72$   $\mu\text{M}$ ) than MDA-MB-231 cells ( $\text{IC}_{50}$  range:  $6.86 \pm 0.31$ – $40.92 \pm 1.59$   $\mu\text{M}$ ), except sulfonamide **10a** that exhibited enhanced activity against MDA-MB-231 cells ( $\text{IC}_{50} = 22.85 \pm 0.91$   $\mu\text{M}$ ) than T47D cells

( $\text{IC}_{50} = 33.51 \pm 1.24$   $\mu\text{M}$ ). As for the activity against T47D cells, sulfonamides **4e** and **6d** emerged as the most potent analogues in this study with  $\text{IC}_{50}$  values of  $7.56 \pm 0.29$  and  $2.45 \pm 0.07$   $\mu\text{M}$ , respectively. Besides, **6d** was the most efficient anti-proliferative agent herein reported, specifically against MDA-MB-231 cells with  $\text{IC}_{50}$  value of  $6.86 \pm 0.31$   $\mu\text{M}$ .

### 2.5. Cell cycle analysis

The efficient anti-proliferative impact of sulfonamides **4e** and **6d** on breast T-47D cancer cell line (Table 4) prompted a further investigation on their growth inhibitory action. The impact of both sulfonamides **4e** and **6d** on cell cycle distribution, after incubation with T-47D cells at their  $\text{IC}_{50}$  concentration (7.56 and 2.45  $\mu\text{M}$ , respectively) for 24 h, was analyzed by a DNA flow cytometry assay (Fig. 6).

The obtained results highlighted that, compared to control cells, breast cancer T-47D cells treated with **4e** and **6d** were arrested at the G2/M phase with an increase in cell population from 16.59% (control) to 26.83% and 35.47%, respectively. Moreover, the number of cells in the sub-G1 phase was dramatically increased from 2.41% (control) to 12.72% and 18.04%, respectively (Fig. 6).

### 2.6. Annexin V-FITC apoptosis assay

To determine whether the growth inhibitory action of sulfonamides **4e** and **6d** is consistent with the induction of apoptosis suggested by the elevated population of sub-G1 in the treated T-47D cells (Fig. 6), Annexin V-FITC/PI double staining (AV/PI) apoptosis assay was carried out (Fig. 7).

The results of this AV-FITC/PI assay revealed that incubation of T-47D cells with sulfonamides **4e** and **6d** resulted in an induction of apoptosis in these cells, that was evidenced via the marked elevation in the apoptotic cells percentage for the early apoptosis (from

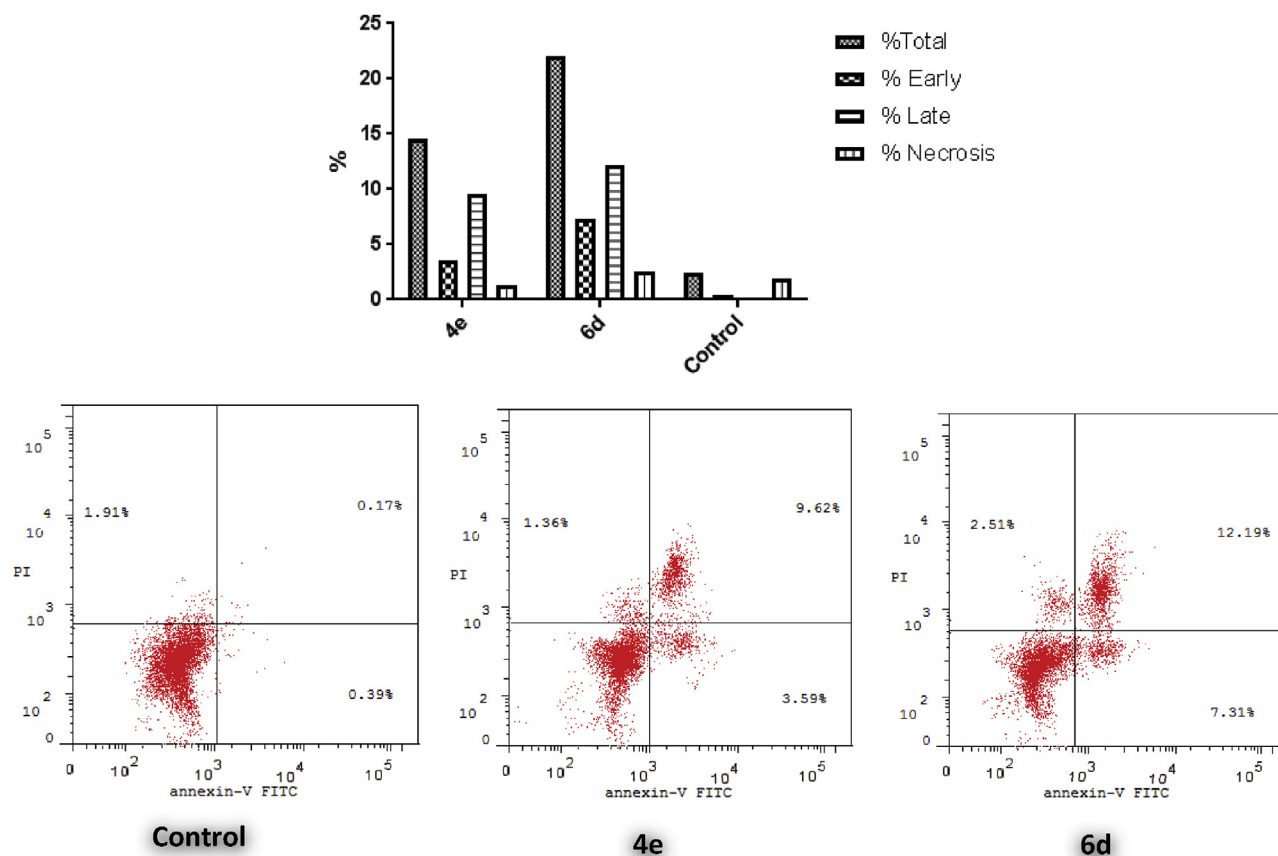


**Fig. 7.** Effect of sulfonamides **4e** and **6d** on the percentage of annexin V-FITC-positive staining in breast T47D cells. The experiments were done in triplicates. The four quadrants identified as: LL, viable; LR, early apoptotic; UR, late apoptotic; UL, necrotic.

0.39% to 3.59% and 7.31, respectively) and the late apoptosis (from 0.17% to 9.62% and 12.19, respectively) phases which represents about 23.6-fold and 34.8-fold total apoptosis increase, compared to the untreated control (Fig. 7).

### 3. Conclusions

The addition of a fluorine atom in the structure of previously reported uracil benzenesulfonamide inhibitors of tumor-associated CAs produced a novel series of derivatives of 5-FU, a widely used medication in the treatment of cancer. A major number of benzenesulfonamide scaffolds as CAIs was here investigated as well as coumarin fragments to achieve a more targeted CA IX/XII inhibition.

Most sulfonamide derivatives efficiently inhibit the target CA IX ( $K_i$ s in the range 0.47–44.7 nM) and CA XII ( $K_i$ s in the range 2.9–83.1 nM), whereas the 5-FU coumarin derivatives **12a–b** and **14** showed a potent and totally selective inhibitory action against the target CA IX/XII over the off-target CA I/II. In contrast, while all sulfonamide compounds exhibited remarkable I/IX and I/XII inhibitory specificity, only two distinct subsets of sulfonamide derivatives produced a preferred inhibition of the target CA IX and XII over the main off-target CA II. When applicable, the comparison of  $K_i$  against CA I, II and IX between a 5-FU derivative and the corresponding nonfluorinated analog previously reported showed that the incorporation of a fluorine atom in position 5 of the nitrogenous base scaffold increases both potency and selectivity against the target CA IX.

The X-ray solved crystal structure of CA II in adduct with a

representative uracil derivative provided insights on the binding mode to the target of such pyrimidine derivatives.

Coumarin **12a**, the sulfonamide CAIs showing the greatest II/IX SI, namely **4e**, **6b** and **6d**, and the unique subnanomolar CA IX inhibitor **10a** were chosen for assessing *in vitro* their antiproliferative action against a panel of eight cancer cell lines. The  $IC_{50}$  values, determined against the most susceptible cancer cell lines MDA-MB-231 and T47D, settle in a low to medium micromolar range ( $2.45 \pm 0.07$ – $18.86 \pm 0.72$   $\mu$ M and  $6.86 \pm 0.31$ – $40.92 \pm 1.59$   $\mu$ M, respectively). A cell cycle analysis showed that **4e** and **6d**, the most active compounds, arrested T-47D cells mainly in the G2/M phase. Using an annexin V-FITC apoptosis assay, **4e** and **6d** were shown to induce an approximately 23.6-fold and 34.8-fold total increase in apoptosis compared to the control, corroborating the concrete potential of these 5-FU CAIs for the design of new effective anti-cancer strategies.

### 4. Experimental section

#### 4.1. Chemistry

Anhydrous solvents and all reagents were purchased from Sigma-Aldrich, Fluorochem and TCI. All reactions involving air- or moisture-sensitive compounds were performed under a nitrogen atmosphere using dried glassware and syringes techniques to transfer solutions. Nuclear magnetic resonance ( $^1H$  NMR,  $^{13}C$  NMR,  $^{19}F$  NMR) spectra were recorded using a Bruker Advance III 400 MHz spectrometer in  $DMSO-d_6$ . Chemical shifts are reported in parts per million (ppm) and the coupling constants ( $J$ ) are

expressed in Hertz (Hz). Splitting patterns are designated as follows: s, singlet; d, doublet; sept, septet; t, triplet; q, quadruplet; m, multiplet; bs, broad singlet; dd, double of doublets. The assignment of exchangeable protons (OH and NH) was confirmed by the addition of D<sub>2</sub>O. Two tautomeric forms of the amide bond were detected for compounds **6a-f** which partially double the signals in the <sup>1</sup>H and <sup>13</sup>C NMR spectra.

Analytical thin-layer chromatography (TLC) was carried out on Sigma Aldrich silica gel F-254 plates. Flash chromatography purifications were performed on Sigma Aldrich Silica gel 60 (230–400 mesh ASTM) as the stationary phase and ethyl acetate/n-hexane or MeOH/DCM were used as eluents. Melting points (mp) were measured in open capillary tubes with a Gallenkamp MPD350.BM3.5 apparatus and are uncorrected. The solvents used in MS measures were acetone, acetonitrile (Chromasolv grade), purchased from Sigma-Aldrich (Milan - Italy), and mQ water 18 MΩ, obtained from Millipore's Simplicity system (Milan-Italy). The mass spectra were obtained using a Varian 1200L triple quadrupole system (Palo Alto, CA, USA) equipped by Electrospray Source (ESI) operating in both positive and negative ions. Stock solutions of analytes were prepared in acetone at 1.0 mg/mL and stored at 4 °C. Working solutions of each analyte were freshly prepared by diluting stock solutions in a mixture of mQ water:acetonitrile 1:1 (v/v) up to a concentration of 1.0 µg mL<sup>-1</sup>. The mass spectra of each analyte were acquired by introducing, via syringe pump at 10 µL min<sup>-1</sup>, the working solution. Raw-data were collected and processed by Varian Workstation Vers. 6.8 software.

#### 4.1.1. Synthesis of 2-(5-fluoro-2,4-dioxo-3,4-dihydropyrimidin-1(2H)-yl)acetic acid **2**

An aqueous solution of chloroacetic acid (1.1 eq in 4 ml of water) was added dropwise to a solution of 5-fluorouracil **1** (1.0 g, 1.0 eq) and KOH (3.0 eq) in water (4 ml) at 100 °C. The reaction mixture was stirred for 2h at the same temperature, then cooled to r.t. and acidified to pH 2. The formed precipitate was collected by filtration and washed with water and Et<sub>2</sub>O. The crude solid was recrystallized from the minimum amount of water to obtain the titled compound as a white powder. 82% yield; m.p. 280–282 °C; silica gel TLC R<sub>f</sub> 0.05 (MeOH/CHCl<sub>3</sub> 10% v/v); δ<sub>H</sub> (400 MHz, DMSO-d<sub>6</sub>): 13.29 (s, 1H, exchange with D<sub>2</sub>O, COOH), 11.96 (s, 1H, exchange with D<sub>2</sub>O, CONHCO), 8.12 (d, J = 6.7 Hz, 1H, Ar-H), 4.40 (s, 2H, CH<sub>2</sub>); δ<sub>C</sub> (100 MHz, DMSO-d<sub>6</sub>): 170.32, 158.51 (d, J<sub>2 CF</sub> = 25.8 Hz), 150.72, 140.38 (d, J<sub>2 CF</sub> = 228.9 Hz), 131.56 (d, J<sub>2 CF</sub> = 33.9 Hz), 49.70; δ<sub>F</sub> (376 MHz, DMSO-d<sub>6</sub>): 170.04 (s); m/z (ESI negative) calcd for C<sub>6</sub>H<sub>4</sub>FN<sub>2</sub>O<sub>4</sub> [M – H]<sup>-</sup> 187.0, found 186.9.

#### 4.1.2. General synthetic procedure of benzenesulfonamides **4a-4e**

EDCI (2.0 eq) was added to a solution of 1-carboxymethyl 5-fluorouracil **2** (0.2 g, 1.0 eq), HOBt (0.5 eq) and DMAP (0.03 eq) in dry DMF (2 ml) under a nitrogen atmosphere and the reaction mixture was stirred at r.t. until the consumption of the starting material (TLC monitoring). Thereafter the proper amino-benzenesulfonamide **3a-3e** (1.1 eq) was added to the reaction mixture, that was stirred at r.t. until the disappearance of the activated ester was observed (TLC monitoring) and then quenched with ice and HCl<sub>(aq)</sub> 2M. The formed precipitate was filtered under *vacuo* and recrystallized from the minimum amount of water to afford the titled compounds as white powders.

4.1.2.1. 2-(5-Fluoro-2,4-dioxo-3,4-dihydropyrimidin-1(2H)-yl)-N-(4-sulfamoylphenyl)acetamide **4a**. Compound **4a** was obtained according the general procedure earlier reported using 1-carboxymethyl 5-fluorouracil **2** (0.2 g, 1.0 eq), HOBt (0.5 eq), DMAP (0.03 eq) and 4-aminobenzenesulfonamide **3a** (1.1 eq) in dry DMF (2 ml). 36% yield; m.p. >300 °C; silica gel TLC R<sub>f</sub> 0.50 (MeOH/

CH<sub>2</sub>Cl<sub>2</sub> 10% v/v); δ<sub>H</sub> (400 MHz, DMSO-d<sub>6</sub>): 11.98 (s, 1H, exchange with D<sub>2</sub>O, CONHCO), 10.67 (s, 1H, exchange with D<sub>2</sub>O, CONH), 8.14 (d, J = 6.7 Hz, 1H, Ar-H), 7.82 (d, J = 8.7 Hz, 2H, Ar-H), 7.76 (d, J = 8.8 Hz, 2H, Ar-H), 7.31 (s, 2H, exchange with D<sub>2</sub>O, SO<sub>2</sub>NH<sub>2</sub>), 4.57 (s, 2H, CH<sub>2</sub>); δ<sub>C</sub> (100 MHz, DMSO-d<sub>6</sub>): 166.89, 158.46 (d, J<sub>2 CF</sub> = 25.7 Hz), 150.74, 142.26, 140.21 (d, J<sub>2 CF</sub> = 228.6 Hz), 139.70, 131.97 (d, J<sub>2 CF</sub> = 34.0 Hz), 127.78, 119.70, 51.22; δ<sub>F</sub> (376 MHz, DMSO-d<sub>6</sub>): 170.40 (d, J = 5.7 Hz); m/z (ESI negative) calcd for C<sub>12</sub>H<sub>10</sub>FN<sub>4</sub>O<sub>5</sub> [M – H]<sup>-</sup> 341.0, found 341.1.

4.1.2.2. 2-(5-Fluoro-2,4-dioxo-3,4-dihydropyrimidin-1(2H)-yl)-N-(3-sulfamoylphenyl)acetamide **4b**. Compound **4b** was obtained according the general procedure earlier reported using 1-carboxymethyl 5-fluorouracil **2** (0.2 g, 1.0 eq), HOBt (0.5 eq), DMAP (0.03 eq) and 3-aminobenzenesulfonamide **3b** (1.1 eq) in dry DMF (2 ml). 54% yield; m.p. >300 °C; silica gel TLC R<sub>f</sub> 0.25 (MeOH/CH<sub>2</sub>Cl<sub>2</sub> 20% v/v); δ<sub>H</sub> (400 MHz, DMSO-d<sub>6</sub>): 11.97 (s, 1H, exchange with D<sub>2</sub>O, CONHCO), 10.62 (s, 1H, exchange with D<sub>2</sub>O, CONH), 8.18 (d, J = 15.2 Hz, 1H, Ar-H), 8.14 (d, J = 6.5 Hz, 1H, Ar-H), 7.74 (s, 1H, Ar-H), 7.57 (s, 2H, Ar-H), 7.42 (s, 2H, exchange with D<sub>2</sub>O, SO<sub>2</sub>NH<sub>2</sub>), 4.56 (s, 2H, CH<sub>2</sub>); δ<sub>C</sub> (100 MHz, DMSO-d<sub>6</sub>): 166.73, 158.47 (d, J<sub>2 CF</sub> = 25.8 Hz), 150.74, 145.70, 140.22 (d, J<sub>2 CF</sub> = 228.5 Hz), 139.72, 131.98 (d, J<sub>2 CF</sub> = 34.0 Hz), 130.57, 122.92, 121.62, 117.16, 51.19; δ<sub>F</sub> (376 MHz, DMSO-d<sub>6</sub>): 170.44 (d, J = 3.3 Hz); m/z (ESI negative) calcd for C<sub>12</sub>H<sub>10</sub>FN<sub>4</sub>O<sub>5</sub> [M – H]<sup>-</sup> 341.0, found 341.1.

4.1.2.3. 2-(5-Fluoro-2,4-dioxo-3,4-dihydropyrimidin-1(2H)-yl)-N-(4-sulfamoylbenzyl)acetamide **4c**. Compound **4c** was obtained according the general procedure earlier reported using 1-carboxymethyl 5-fluorouracil **2** (0.2 g, 1.0 eq), HOBt (0.5 eq), DMAP (0.03 eq) and 4-(aminomethyl)benzenesulfonamide hydrochloride **3c** (1.1 eq) and DIPEA (1.1 eq) in dry DMF (2 ml). 25% yield; m.p. >300 °C; silica gel TLC R<sub>f</sub> 0.30 (MeOH/CH<sub>2</sub>Cl<sub>2</sub> 10% v/v); δ<sub>H</sub> (400 MHz, DMSO-d<sub>6</sub>): 11.87 (s, 1H, exchange with D<sub>2</sub>O, CONHCO), 8.79 (t, J = 5.8 Hz, 1H, exchange with D<sub>2</sub>O, CONH), 8.10 (d, J = 6.8 Hz, 1H, Ar-H), 7.80 (d, J = 8.2 Hz, 2H, Ar-H), 7.47 (d, J = 8.2 Hz, 2H, Ar-H), 7.35 (s, 2H, exchange with D<sub>2</sub>O, SO<sub>2</sub>NH<sub>2</sub>), 4.41 (d, J = 5.8 Hz, 2H, CH<sub>2</sub>), 4.38 (s, 2H, CH<sub>2</sub>); δ<sub>C</sub> (100 MHz, DMSO-d<sub>6</sub>): 167.78, 158.68 (d, J<sub>2 CF</sub> = 27.2 Hz), 150.74, 144.04, 143.65, 140.40 (d, J<sub>2 CF</sub> = 238.7 Hz), 131.82 (d, J<sub>2 CF</sub> = 45.1 Hz), 128.45, 126.58, 50.86, 42.75; δ<sub>F</sub> (376 MHz, DMSO-d<sub>6</sub>): 170.46 (d, J = 3.7 Hz); m/z (ESI negative) calcd for C<sub>13</sub>H<sub>12</sub>FN<sub>4</sub>O<sub>5</sub> [M – H]<sup>-</sup> 355.1, found 355.0.

4.1.2.4. 2-(5-Fluoro-2,4-dioxo-3,4-dihydropyrimidin-1(2H)-yl)-N-(4-sulfamoylphenethyl)acetamide **4d**. Compound **4d** was obtained according the general procedure earlier reported using 1-carboxymethyl 5-fluorouracil **2** (0.2 g, 1.0 eq), HOBt (0.5 eq), DMAP (0.03 eq) and 4-(aminoethyl)benzenesulfonamide **3d** (1.1 eq) in dry DMF (2 ml). 63% yield; m.p. 258–260 °C; silica gel TLC R<sub>f</sub> 0.55 (MeOH/CH<sub>2</sub>Cl<sub>2</sub> 10% v/v); δ<sub>H</sub> (400 MHz, DMSO-d<sub>6</sub>): 11.88 (s, 1H, exchange with D<sub>2</sub>O, CONHCO), 8.33 (t, J = 5.3 Hz, 1H, exchange with D<sub>2</sub>O, CONH), 8.05 (d, J = 6.7 Hz, 1H, Ar-H), 7.78 (d, J = 8.2 Hz, 2H, Ar-H), 7.45 (d, J = 8.2 Hz, 2H, Ar-H), 7.34 (s, 2H, exchange with D<sub>2</sub>O, SO<sub>2</sub>NH<sub>2</sub>), 4.28 (s, 2H, CH<sub>2</sub>), 3.35 (d, J = 15.0 Hz, 2H, CH<sub>2</sub>), 2.80 (dd, J = 31.9, 24.9 Hz, 2H, CH<sub>2</sub>); δ<sub>C</sub> (100 MHz, DMSO-d<sub>6</sub>): 167.50, 158.60 (d, J<sub>2 CF</sub> = 35.1 Hz), 150.65, 144.43, 143.05, 140.23 (d, J<sub>2 CF</sub> = 234.2 Hz), 131.99 (d, J<sub>2 CF</sub> = 35.9 Hz), 130.11, 126.63, 50.61, 35.54; δ<sub>F</sub> (376 MHz, DMSO-d<sub>6</sub>): 170.66 (s); m/z (ESI negative) calcd for C<sub>14</sub>H<sub>14</sub>FN<sub>4</sub>O<sub>5</sub> [M – H]<sup>-</sup> 369.1, found 369.0.

4.1.2.5. 2-(5-Fluoro-2,4-dioxo-3,4-dihydropyrimidin-1(2H)-yl)-N-(2-hydroxy-5-sulfamoylphenyl)acetamide **4e**. Compound **4e** was obtained according the general procedure earlier reported using 1-carboxymethyl 5-fluorouracil **2** (0.2 g, 1.0 eq), HOBt (0.5 eq), DMAP (0.03 eq) and 3-amino-4-hydroxybenzenesulfonamide **3e**

(1.1 eq) in dry DMF (2 ml), 46% yield; m.p. >300 °C; silica gel TLC  $R_f$  0.20 (MeOH/CH<sub>2</sub>Cl<sub>2</sub> 10% v/v);  $\delta_H$  (400 MHz, DMSO-*d*<sub>6</sub>): 11.92 (s, 1H, exchange with D<sub>2</sub>O, CONHCO), 10.85 (s, 1H, Ar-H), 9.82 (s, 1H, exchange with D<sub>2</sub>O, OH), 8.49 (s, 1H, exchange with D<sub>2</sub>O, CONH), 8.13 (d,  $J$  = 6.6 Hz, 1H, Ar-H), 7.45 (d,  $J$  = 8.1 Hz, 1H, Ar-H), 7.16 (s, 2H, exchange with D<sub>2</sub>O, SO<sub>2</sub>NH<sub>2</sub>), 7.03 (d,  $J$  = 8.4 Hz, 1H, Ar-H), 4.71 (d,  $J$  = 52.0 Hz, 2H, CH<sub>2</sub>);  $\delta_C$  (100 MHz, DMSO-*d*<sub>6</sub>): 166.85, 158.45 (d,  $J_{2CF}$  = 25.7 Hz), 151.30, 150.74, 140.17 (d,  $J_{2CF}$  = 227.7 Hz), 135.53, 132.07 (d,  $J_{2CF}$  = 33.5 Hz), 126.63, 123.56, 120.60, 115.59, 51.24;  $\delta_F$  (376 MHz, DMSO-*d*<sub>6</sub>): 170.64 (d,  $J$  = 14.1 Hz);  $m/z$  (ESI negative) calcd for C<sub>12</sub>H<sub>10</sub>FN<sub>4</sub>O<sub>6</sub>S [M - H]<sup>-</sup> 357.0, found 356.9.

#### 4.1.3. General synthetic procedure of benzenesulfonamides 6a-6f

EDCI (2.0 eq) was added to a solution of 1-carboxymethyl 5-fluorouracil **2** (0.2 g, 1.0 eq), HOBT (0.5 eq) and DMAP (0.03 eq) in dry DMF (2 ml) under a nitrogen atmosphere and the reaction mixture was stirred at r.t. until the consumption of the starting material (TLC monitoring). Thereafter the proper amino-benzenesulfonamide **5a-5f** (1.5 eq) was added to the reaction mixture, that was stirred at r.t. until the disappearance of the activated ester was observed (TLC monitoring) and then quenched with ice and HCl<sub>(aq)</sub> 2M. The collected, water washed precipitate was triturated in MeOH to afford the pure titled compounds as powders.

**4.1.3.1. N-benzyl-2-(5-fluoro-2,4-dioxo-3,4-dihydropyrimidin-1(2H)-yl)-N-(4-sulfamoylphenethyl)acetamide 6a.** Compound **6a** was obtained according the general procedure earlier reported using 1-carboxymethyl 5-fluorouracil **2** (0.2 g, 1.0 eq), HOBT (0.5 eq), DMAP (0.03 eq) and 4-(2-(benzylamino)ethyl)benzenesulfonamide **5a** (1.1 eq) in dry DMF (2 ml). 23% yield; m.p. 234–236 °C; silica gel TLC  $R_f$  0.75 (MeOH/CH<sub>2</sub>Cl<sub>2</sub> 15% v/v);  $\delta_H$  (400 MHz, DMSO-*d*<sub>6</sub>): 11.87 (s, 1H, exchange with D<sub>2</sub>O, CONHCO), 8.09 (d,  $J$  = 6.8 Hz, 0.5H, Ar-H), 8.04 (d,  $J$  = 6.7 Hz, 0.5H, Ar-H), 7.80 (d,  $J$  = 8.1 Hz, 1H, Ar-H), 7.77 (d,  $J$  = 8.1 Hz, 1H, Ar-H), 7.51 (d,  $J$  = 8.2 Hz, 2H, Ar-H), 7.43 (m, 7H, partially exchange with D<sub>2</sub>O, Ar-H + SONH<sub>2</sub>), 4.72 (s, 1H, CH<sub>2</sub>), 4.67 (s, 1H, CH<sub>2</sub>), 4.60 (s, 1H, CH<sub>2</sub>), 4.57 (s, 1H, CH<sub>2</sub>), 3.48 (m, 2H, CH<sub>2</sub>), 3.02 (m, 1H, CH<sub>2</sub>), 2.84 (m, 1H, CH<sub>2</sub>);  $\delta_C$  (100 MHz, DMSO-*d*<sub>6</sub>): 167.47, 161.16, 158.57 (d,  $J_{2CF}$  = 26.3 Hz), 150.82, 143.36, 140.39 (d,  $J_{2CF}$  = 544.7 Hz), 138.41, 130.27, 129.82 (d,  $J_{2CF}$  = 32.7 Hz), 129.38, 128.62, 128.10, 126.78, 50.94, 49.44 (d,  $J_{2CF}$  = 28.2 Hz), 48.38 (d,  $J_{2CF}$  = 15.2 Hz), 34.22 (d,  $J_{2CF}$  = 95.9 Hz);  $\delta_F$  (376 MHz, DMSO-*d*<sub>6</sub>): 170.62;  $m/z$  (ESI negative) calcd for C<sub>21</sub>H<sub>20</sub>FN<sub>4</sub>O<sub>5</sub>S [M - H]<sup>-</sup> 459.1, found 459.1.

**4.1.3.2. N-(4-Chlorobenzyl)-2-(5-fluoro-2,4-dioxo-3,4-dihydropyrimidin-1(2H)-yl)-N-(4-sulfamoylphenethyl)acetamide 6b.** Compound **6b** was obtained according the general procedure earlier reported using 1-carboxymethyl 5-fluorouracil **2** (0.2 g, 1.0 eq), HOBT (0.5 eq), DMAP (0.03 eq) and 4-(2-((4-chlorobenzyl)amino)ethyl)benzenesulfonamide **5b** (1.1 eq) in dry DMF (2 ml). 65% yield; m.p. 260–262 °C; silica gel TLC  $R_f$  0.80 (MeOH/CH<sub>2</sub>Cl<sub>2</sub> 20% v/v);  $\delta_H$  (400 MHz, DMSO-*d*<sub>6</sub>): 11.86 (s, 1H, exchange with D<sub>2</sub>O, CONHCO), 8.09 (d,  $J$  = 6.7 Hz, 0.5H, Ar-H), 8.04 (d,  $J$  = 6.7 Hz, 0.5H, Ar-H), 7.81 (d,  $J$  = 8.2 Hz, 1H, Ar-H), 7.77 (d,  $J$  = 8.2 Hz, 1H, Ar-H), 7.53 (d,  $J$  = 8.2 Hz, 1H, Ar-H), 7.50 (d,  $J$  = 8.4 Hz, 1H, Ar-H), 7.42 (m, 3H, Ar-H), 7.33 (m, 3H, partially exchange with D<sub>2</sub>O, Ar-H + SONH<sub>2</sub>), 4.72 (s, 1H, CH<sub>2</sub>), 4.64 (s, 1H, CH<sub>2</sub>), 4.62 (s, 1H, CH<sub>2</sub>), 4.56 (s, 1H, CH<sub>2</sub>), 3.53 (m, 1H, CH<sub>2</sub>), 3.46 (m, 1H, CH<sub>2</sub>), 3.03 (m, 1H, CH<sub>2</sub>), 2.86 (m, 1H, CH<sub>2</sub>);  $\delta_C$  (100 MHz, DMSO-*d*<sub>6</sub>): 167.62, 158.48 (d,  $J_{2CF}$  = 23.7 Hz), 150.72, 143.32, 140.25 (d,  $J_{2CF}$  = 243.4 Hz), 137.52, 132.86 (d,  $J_{2CF}$  = 39.0 Hz), 130.52, 130.28, 129.97, 129.59, 129.32, 126.78, 50.03 (d,  $J_{2CF}$  = 41.8 Hz), 49.20 (d,  $J_{2CF}$  = 65.6 Hz), 48.45, 34.20 (d,  $J_{2CF}$  = 108.8 Hz);  $\delta_F$  (376 MHz, DMSO-*d*<sub>6</sub>): 170.59;  $m/z$  (ESI negative) calcd for C<sub>21</sub>H<sub>19</sub>ClFN<sub>4</sub>O<sub>5</sub>S [M - H]<sup>-</sup> 493.1, found 493.0.

#### 4.1.3.3. 2-(5-Fluoro-2,4-dioxo-3,4-dihydropyrimidin-1(2H)-yl)-N-(4-fluorobenzyl)-N-(4-sulfamoylphenethyl)acetamide 6c.

Compound **6c** was obtained according the general procedure earlier reported using 1-carboxymethyl 5-fluorouracil **2** (0.2 g, 1.0 eq), HOBT (0.5 eq), DMAP (0.03 eq) and 4-(2-((4-fluorobenzyl)amino)ethyl)benzenesulfonamide **5c** (1.1 eq) in dry DMF (2 ml). 65% yield; m.p. 257–259 °C; silica gel TLC  $R_f$  0.83 (MeOH/CH<sub>2</sub>Cl<sub>2</sub> 20% v/v);  $\delta_H$  (400 MHz, DMSO-*d*<sub>6</sub>): 11.91 (s, 1H, exchange with D<sub>2</sub>O, CONHCO), 8.08 (d,  $J$  = 6.8 Hz, 0.5H, Ar-H), 8.02 (d,  $J$  = 6.7 Hz, 0.5H, Ar-H), 7.80 (d,  $J$  = 8.2 Hz, 1H, Ar-H), 7.77 (d,  $J$  = 8.2 Hz, 1H, Ar-H), 7.52 (d,  $J$  = 8.2 Hz, 1H, Ar-H), 7.32 (m, 7H, partially exchange with D<sub>2</sub>O, Ar-H + SONH<sub>2</sub>), 4.70 (s, 1H, CH<sub>2</sub>), 4.66 (s, 1H, CH<sub>2</sub>), 4.59 (s, 1H, CH<sub>2</sub>), 4.55 (s, 1H, CH<sub>2</sub>), 3.48 (m, 2H, CH<sub>2</sub>), 3.01 (m, 1H, CH<sub>2</sub>), 2.84 (m, 1H, CH<sub>2</sub>);  $\delta_C$  (100 MHz, DMSO-*d*<sub>6</sub>): 167.55, 158.65 (d,  $J_{2CF}$  = 14.0 Hz), 150.73, 143.99, 143.26 (d,  $J_{2CF}$  = 22.8 Hz), 140.23 (d,  $J_{2CF}$  = 212.0 Hz), 132.00 (d,  $J_{2CF}$  = 40.0 Hz), 130.72 (d,  $J_{2CF}$  = 7.9 Hz), 130.27, 129.98, 126.79, 116.53, 116.01, 50.04 (d,  $J_{2CF}$  = 34.5 Hz), 49.12 (d,  $J_{2CF}$  = 77.7 Hz), 48.28, 34.18 (d,  $J_{2CF}$  = 112.8 Hz);  $\delta_F$  (376 MHz, DMSO-*d*<sub>6</sub>): 115.29, -170.13;  $m/z$  (ESI negative) calcd for C<sub>21</sub>H<sub>19</sub>F<sub>2</sub>N<sub>4</sub>O<sub>5</sub>S [M - H]<sup>-</sup> 477.1, found 477.2.

#### 4.1.3.4. 2-(5-Fluoro-2,4-dioxo-3,4-dihydropyrimidin-1(2H)-yl)-N-(4-methoxybenzyl)-N-(4-sulfamoylphenethyl)acetamide 6d.

Compound **6d** was obtained according the general procedure earlier reported using 1-carboxymethyl 5-fluorouracil **2** (0.2 g, 1.0 eq), HOBT (0.5 eq), DMAP (0.03 eq) and 4-(2-((4-methoxybenzyl)amino)ethyl)benzenesulfonamide **5d** (1.1 eq) in dry DMF (2 ml). 69% yield; m.p. 210–212 °C; silica gel TLC  $R_f$  0.63 (MeOH/CH<sub>2</sub>Cl<sub>2</sub> 20% v/v);  $\delta_H$  (400 MHz, DMSO-*d*<sub>6</sub>): 11.88 (s, 1H, exchange with D<sub>2</sub>O, CONHCO), 8.07 (d,  $J$  = 6.8 Hz, 0.5H, Ar-H), 8.00 (d,  $J$  = 6.7 Hz, 0.5H, Ar-H), 7.77 (d,  $J$  = 8.2 Hz, 1H, Ar-H), 7.74 (d,  $J$  = 8.2 Hz, 1H, Ar-H), 7.48 (d,  $J$  = 8.2 Hz, 1H, Ar-H), 7.35 (d,  $J$  = 8.2 Hz, 1H, Ar-H), 7.29 (s, 2H, exchange with D<sub>2</sub>O, SO<sub>2</sub>NH<sub>2</sub>), 7.28 (d,  $J$  = 8.2 Hz, 1H, Ar-H), 7.21 (d,  $J$  = 8.5 Hz, 1H, Ar-H), 6.96 (d,  $J$  = 8.6 Hz, 1H, Ar-H), 6.90 (d,  $J$  = 8.6 Hz, 1H, Ar-H), 4.65 (s, 2H, CH<sub>2</sub>), 4.48 (s, 1H, CH<sub>2</sub>), 4.46 (s, 1H, CH<sub>2</sub>), 3.76 (s, 1.5H, CH<sub>2</sub>), 3.74 (s, 1.5H, CH<sub>2</sub>), 3.44 (m, 2H, CH<sub>2</sub>), 2.96 (m, 1H, CH<sub>2</sub>), 2.79 (m, 1H, CH<sub>2</sub>);  $\delta_C$  (100 MHz, DMSO-*d*<sub>6</sub>): 167.45, 159.75 (d,  $J_{2CF}$  = 8.6 Hz), 150.86, 144.20, 143.53 (d,  $J_{2CF}$  = 9.2 Hz), 143.26, 135.71 (d,  $J_{2CF}$  = 243.0 Hz), 130.39, 130.11, 129.73, 126.92, 115.18, 114.94, 56.13, 49.79 (d,  $J_{2CF}$  = 31.0 Hz), 48.73, 48.17 (d,  $J_{2CF}$  = 21.2 Hz), 34.31 (d,  $J_{2CF}$  = 104.7 Hz);  $\delta_F$  (376 MHz, DMSO-*d*<sub>6</sub>): 170.66;  $m/z$  (ESI negative) calcd for C<sub>22</sub>H<sub>22</sub>FN<sub>4</sub>O<sub>6</sub>S [M - H]<sup>-</sup> 489.1, found 489.0.

#### 4.1.3.5. N-(4-Cyanobenzyl)-2-(5-fluoro-2,4-dioxo-3,4-dihydropyrimidin-1(2H)-yl)-N-(4-sulfamoylphenethyl)acetamide 6e.

Compound **6e** was obtained according the general procedure earlier reported using 1-carboxymethyl 5-fluorouracil **2** (0.2 g, 1.0 eq), HOBT (0.5 eq), DMAP (0.03 eq) and 4-(2-((4-cyanobenzyl)amino)ethyl)benzenesulfonamide **5e** (1.1 eq) in dry DMF (2 ml). 43% yield; m.p. 230–232 °C; silica gel TLC  $R_f$  0.60 (MeOH/CH<sub>2</sub>Cl<sub>2</sub> 20% v/v);  $\delta_H$  (400 MHz, DMSO-*d*<sub>6</sub>): 11.92 (s, 1H, exchange with D<sub>2</sub>O, CONHCO), 8.02 (d,  $J$  = 6.7 Hz, 0.5H, Ar-H), 7.99 (d,  $J$  = 6.7 Hz, 0.5H, Ar-H), 7.86 (d,  $J$  = 8.2 Hz, 1H, Ar-H), 7.74 (m, 3H, Ar-H), 7.49 (m, 3H, Ar-H), 7.43 (d,  $J$  = 8.1 Hz, 1H, Ar-H), 7.36 (d,  $J$  = 8.2 Hz, 1H, Ar-H), 7.27 (s, 2H, exchange with D<sub>2</sub>O, SO<sub>2</sub>NH<sub>2</sub>), 4.70 (s, 2H, CH<sub>2</sub>), 4.62 (s, 1H, CH<sub>2</sub>), 4.56 (s, 1H, CH<sub>2</sub>), 3.53 (m, 1H, CH<sub>2</sub>), 3.44 (m, 1H, CH<sub>2</sub>), 2.98 (m, 1H, CH<sub>2</sub>), 2.82 (m, 1H, CH<sub>2</sub>);  $\delta_C$  (100 MHz, DMSO-*d*<sub>6</sub>): 167.99, 158.68 (d,  $J_{2CF}$  = 35.5 Hz), 150.86, 144.59, 143.92 (d,  $J_{2CF}$  = 14.9 Hz), 140.33 (d,  $J_{2CF}$  = 258.6 Hz), 133.70, 133.42, 130.46, 129.37, 126.91, 119.91, 111.00, 50.40 (d,  $J_{2CF}$  = 96.5 Hz), 49.65, 49.01 (d,  $J_{2CF}$  = 8.1 Hz), 34.35 (d,  $J_{2CF}$  = 111.3 Hz);  $\delta_F$  (376 MHz, DMSO-*d*<sub>6</sub>): 170.34;  $m/z$  (ESI negative) calcd for C<sub>22</sub>H<sub>19</sub>FN<sub>5</sub>O<sub>5</sub>S [M - H]<sup>-</sup> 484.1, found 484.2.

4.1.3.6. *N*-(4-(Dimethylamino)benzyl)-2-(5-fluoro-2,4-dioxo-3,4-dihydropyrimidin-1(2H)-yl)-*N*-(4-sulfamoylphenethyl)acetamide **6f**. Compound **6f** was obtained according the general procedure earlier reported using 1-carboxymethyl 5-fluorouracil **2** (0.2 g, 1.0 eq), HOBt (0.5 eq), DMAP (0.03 eq) and 4-(2-((4-(dimethylamino)benzyl)amino)ethyl)benzenesulfonamide **5f** (1.1 eq) in dry DMF (2 ml). 28% yield; m.p. 188–190 °C; silica gel TLC  $R_f$  0.78 (MeOH/CH<sub>2</sub>Cl<sub>2</sub> 20% v/v);  $\delta_H$  (400 MHz, DMSO-*d*<sub>6</sub>): 11.93 (s, 1H, exchange with D<sub>2</sub>O, CONHCO), 9.24 (s, 1H, Ar-*H*), 7.82 (d, *J* = 7.7 Hz, 2H, Ar-*H*), 7.47 (d, *J* = 8.1 Hz, 2H, Ar-*H*), 7.36 (m, 4H, partially exchange with D<sub>2</sub>O, Ar-*H* + SO<sub>2</sub>NH<sub>2</sub>), 6.77 (d, *J* = 7.5 Hz, 2H, Ar-*H*), 4.68 (s, 1H, CH<sub>2</sub>), 4.43 (s, 1H, CH<sub>2</sub>), 4.06 (s, 2H, CH<sub>2</sub>), 3.11 (s, 2H, CH<sub>2</sub>), 2.95 (s, 6H, 2 x CH<sub>3</sub>), 2.90 (m, 1H, CH<sub>2</sub>), 2.79 (m, 1H, CH<sub>2</sub>);  $\delta_C$  (100 MHz, DMSO-*d*<sub>6</sub>): 167.27, 151.79, 150.80 (d,  $J_{CF}$  = 13.9 Hz), 143.79, 143.37 (d,  $J_{CF}$  = 20.3 Hz), 142.47, 138.05 (d,  $J_{CF}$  = 215.0 Hz), 132.16, 130.21, 127.05, 126.88, 119.52, 113.05, 50.82, 49.86 (d,  $J_{CF}$  = 36.8 Hz), 48.47 (d,  $J_{CF}$  = 58.6 Hz), 47.56, 33.01 (d,  $J_{CF}$  = 160.3 Hz);  $\delta_F$  (376 MHz, DMSO-*d*<sub>6</sub>): 170.70; *m/z* (ESI negative) calcd for C<sub>23</sub>H<sub>25</sub>FN<sub>5</sub>O<sub>5</sub>S [M – H]<sup>–</sup> 502.2, found 502.1.

#### 4.1.4. General synthetic procedure of azides

The proper amine **3a**, **3b**, **8a**, **8b**, **11a** (0.5 g, 1.0 eq) was dissolved in a 2M HCl aqueous solution (5 ml). NaNO<sub>2</sub> (1.2 eq) was slowly added at 0 °C and the reaction mixture was stirred at the same temperature for 0.5h. Thereafter NaN<sub>3</sub> (1.5 eq) was added portion-wise and the mixture was stirred at r.t. for 0.5h. The obtained precipitate was filtered-off and washed with water to afford the corresponding azides **9a–9d** and **13**.

4.1.4.1. *4-Azido-benzenesulfonamide 9a*. Compound **9a** was obtained according the general procedure earlier reported 4-aminobenzenesulfonamide **3a** (0.5 g, 1.0 eq), NaNO<sub>2</sub> (1.2 eq) and NaN<sub>3</sub> (1.5 eq) in a HCl 2M aqueous solution. 63% yield; m.p. 120–121 °C; silica gel TLC  $R_f$  0.47 (EtOAc/*n*-hexane 50% v/v);  $\delta_H$  (400 MHz, DMSO-*d*<sub>6</sub>): 7.33 (d, *J* = 8.8, 2H, Ar), 7.41 (s, 2H, exchange with D<sub>2</sub>O, SO<sub>2</sub>NH<sub>2</sub>), 7.87 (d, *J* = 8.8, 2H, Ar);  $\delta_C$  (100 MHz, DMSO-*d*<sub>6</sub>): 120.5, 128.6, 141.5, 143.9; *m/z* (ESI negative) calcd for C<sub>6</sub>H<sub>5</sub>N<sub>4</sub>O<sub>2</sub>S [M – H]<sup>–</sup> 197.0, found 197.1.

4.1.4.2. *3-Azido-benzenesulfonamide 9b*. Compound **9b** was obtained according the general procedure earlier reported 3-aminobenzenesulfonamide **3b** (0.5 g, 1.0 eq), NaNO<sub>2</sub> (1.2 eq) and NaN<sub>3</sub> (1.5 eq) in a HCl 2M aqueous solution. 60% yield; m.p. 110 °C; silica gel TLC  $R_f$  0.35 (EtOAc/*n*-hexane 50% v/v);  $\delta_H$  (400 MHz, DMSO-*d*<sub>6</sub>): 7.37 (m, 2H, Ar-*H*), 7.48 (s, 2H, exchange with D<sub>2</sub>O, SO<sub>2</sub>NH<sub>2</sub>), 7.52 (s, 1H, Ar-*H*), 7.63 (m, 1H, Ar-*H*);  $\delta_C$  (100 MHz, DMSO-*d*<sub>6</sub>): 117.2, 123.1, 123.5, 131.8, 141.4, 146.9; *m/z* (ESI negative) calcd for C<sub>6</sub>H<sub>5</sub>N<sub>4</sub>O<sub>2</sub>S [M – H]<sup>–</sup> 197.0, found 197.1.

4.1.4.3. *4-Azido-3-chlorobenzenesulfonamide 9c*. Compound **9c** was obtained according the general procedure earlier reported 4-amino-3-chlorobenzenesulfonamide **8a** (0.5 g, 1.0 eq), NaNO<sub>2</sub> (1.2 eq) and NaN<sub>3</sub> (1.5 eq) in a HCl 2M aqueous solution. 65% yield; m.p. 140–142 °C; silica gel TLC  $R_f$  0.38 (MeOH/CH<sub>2</sub>Cl<sub>2</sub> 10% v/v);  $\delta_H$  (400 MHz, DMSO-*d*<sub>6</sub>): 8.23 (s, 1H, Ar-*H*), 7.63 (d, *J* = 8.8, 1H, Ar-*H*), 7.43 (d, *J* = 8.6, 1H, Ar-*H*), 7.23 (s, 2H, exchange with D<sub>2</sub>O, SO<sub>2</sub>NH<sub>2</sub>);  $\delta_C$  (100 MHz, DMSO-*d*<sub>6</sub>): 141.1, 134.6, 130.5, 126.6, 125.4, 105.9; *m/z* (ESI negative) calcd for C<sub>6</sub>H<sub>4</sub>ClN<sub>4</sub>O<sub>2</sub>S [M – H]<sup>–</sup> 231.0, found 230.9.

4.1.4.4. *4-Azido-3-bromobenzenesulfonamide 9d*. Compound **9d** was obtained according the general procedure earlier reported 4-amino-3-bromobenzenesulfonamide **8b** (0.5 g, 1.0 eq), NaNO<sub>2</sub> (1.2 eq) and NaN<sub>3</sub> (1.5 eq) in a HCl 2M aqueous solution. 70% yield; m.p. 154–156 °C; silica gel TLC  $R_f$  0.29 (MeOH/CH<sub>2</sub>Cl<sub>2</sub> 10% v/v);  $\delta_H$  (400 MHz, DMSO-*d*<sub>6</sub>): 8.18 (s, 1H, Ar-*H*), 7.73 (d, *J* = 8.8, 1H, Ar-*H*),

7.38 (d, *J* = 8.6, 1H, Ar-*H*), 7.23 (s, 2H, exchange with D<sub>2</sub>O, SO<sub>2</sub>NH<sub>2</sub>);  $\delta_C$  (100 MHz, DMSO-*d*<sub>6</sub>): 141.9, 134.8, 131.3, 129.5, 126.3, 117.7; *m/z* (ESI negative) calcd for C<sub>6</sub>H<sub>4</sub>BrN<sub>4</sub>O<sub>2</sub>S [M – H]<sup>–</sup> 274.9, found 274.8.

4.1.4.5. *7-Azido-4-methyl-chromen-2-one 13*. Compound **13** was obtained according the general procedure earlier reported 7-amino-4-methyl-chromen-2-one **11a** (0.5 g, 1.0 eq), NaNO<sub>2</sub> (1.2 eq) and NaN<sub>3</sub> (1.5 eq) in a HCl 2M aqueous solution. 88% yield; m.p. 122–124 °C; silica gel TLC  $R_f$  0.57 (EtOAc/*n*-hexane 20% v/v);  $\delta_H$  (400 MHz, DMSO-*d*<sub>6</sub>): 7.83 (d, *J* = 8.4, 1H, Ar-*H*), 7.18 (m, 2H, Ar-*H*), 6.38 (d, *J* = 1.2, 1H, Ar-*H*), 2.46 (d, *J* = 1.2, 3H, CH<sub>3</sub>);  $\delta_C$  (100 MHz, DMSO-*d*<sub>6</sub>): 160.4, 155.0, 153.8, 144.2, 127.9, 117.7, 116.5, 114.1, 107.7, 19.0; *m/z* (ESI positive) calcd for C<sub>10</sub>H<sub>8</sub>N<sub>3</sub>O<sub>2</sub> [M – H]<sup>+</sup> 202.1, found 202.0.

#### 4.1.5. Synthesis of 5-fluoro-1-(prop-2-yn-1-yl)pyrimidine-2,4(1H,3H)-dione **7**

Propargyl bromide (1.0 eq) was added dropwise to a solution of 5-fluorouracil **1** (0.5 g, 1.0 eq) and DBU (1.0 eq) in dry CH<sub>3</sub>CN (7 ml) at 0 °C under a nitrogen atmosphere. The reaction mixture was refluxed for 1.5h, then quenched with HCl(aq) 1M (15 ml) and extracted with EtOAc (25 ml). The organic layer was dried over Na<sub>2</sub>SO<sub>4</sub>, filtered-off and concentrated under *vacuo* to give a residue that was purified by silica gel column chromatography eluting with 40% EtOAc in *n*-hexane to afford the title compound **7** as white solid. 63% yield; m.p. 140–142 °C; silica gel TLC  $R_f$  0.20 (EtOAc/*n*-hexane 40% v/v);  $\delta_H$  (400 MHz, DMSO-*d*<sub>6</sub>): 11.92 (s, 1H, exchange with D<sub>2</sub>O, CONHCO), 8.17 (d, *J* = 6.6 Hz, 1H, Ar-*H*), 4.49 (d, *J* = 2.3 Hz, 2H, CH<sub>2</sub>), 3.48 (t, *J* = 2.3 Hz, 1H, CH);  $\delta_C$  (100 MHz, DMSO-*d*<sub>6</sub>): 158.40 (d,  $J_{CF}$  = 25.9 Hz), 150.12, 140.87 (d,  $J_{CF}$  = 230.5 Hz), 129.96 (d,  $J_{CF}$  = 33.9 Hz), 79.18, 77.18, 38.05;  $\delta_F$  (376 MHz, DMSO-*d*<sub>6</sub>): 168.41; *m/z* (ESI negative) calcd for C<sub>7</sub>H<sub>4</sub>FN<sub>2</sub>O<sub>2</sub> [M – H]<sup>–</sup> 167.0, found 167.1.

#### 4.1.6. General synthetic procedure of triazoles 10a–10d and 14

The proper azide **9a–9d** and **13** (1.1 eq) was added to a solution of propargyl derivate **7** (0.1 g, 1.0 eq) in H<sub>2</sub>O/*t*BuOH 1/1 (8 ml) at r.t., followed by a suspension of CuSO<sub>4</sub> (0.1 eq) and Na ascorbate (0.5 eq) in water (0.5 ml). The reaction mixture was stirred at 40 °C overnight, then quenched with H<sub>2</sub>O (20 ml) and the formed precipitate was collected by filtration *in vacuo*. A solution of the residue in DMF (4 ml) was filtered-off through Celite521® and then poured on slush (20 ml). The precipitate was filtered *in vacuo* and washed with Et<sub>2</sub>O to afford the titled compounds **10a–10d** and **14** as powders.

##### 4.1.6.1. 4-(4-((5-Fluoro-2,4-dioxo-3,4-dihydropyrimidin-1(2H)-yl)methyl)-1H-1,2,3-triazol-1-yl)benzenesulfonamide 10a.

Compound **10a** was obtained according the general procedure earlier reported using 5-fluoro-1-(prop-2-yn-1-yl)pyrimidine-2,4(1H,3H)-dione **7** (0.1 g, 1.0 eq), 4-azidobenzenesulfonamide **9a** (1.1 eq), CuSO<sub>4</sub> (0.1 eq) and Na ascorbate (0.5 eq) in H<sub>2</sub>O/*t*BuOH 1/1 (8 ml). 73% yield; m.p. >300 °C; silica gel TLC  $R_f$  0.20 (MeOH/CH<sub>2</sub>Cl<sub>2</sub> 10% v/v);  $\delta_H$  (400 MHz, DMSO-*d*<sub>6</sub>): 11.94 (s, 1H, exchange with D<sub>2</sub>O, CONHCO), 8.95 (s, 1H, Ar-*H*), 8.28 (d, *J* = 6.7 Hz, 1H, Ar-*H*), 8.16 (d, *J* = 8.7 Hz, 2H, Ar-*H*), 8.05 (d, *J* = 8.6 Hz, 2H, Ar-*H*), 7.57 (s, 2H, exchange with D<sub>2</sub>O, SO<sub>2</sub>NH<sub>2</sub>), 5.06 (s, 2H, CH<sub>2</sub>);  $\delta_C$  (100 MHz, DMSO-*d*<sub>6</sub>): 158.61 (d,  $J_{CF}$  = 25.9 Hz), 150.53, 145.09, 144.98, 140.94 (d,  $J_{CF}$  = 225.6 Hz), 139.56, 130.95 (d,  $J_{CF}$  = 33.7 Hz), 128.57, 123.00, 121.34, 43.86;  $\delta_F$  (376 MHz, DMSO-*d*<sub>6</sub>): 168.94; *m/z* (ESI negative) calcd for C<sub>13</sub>H<sub>10</sub>FN<sub>6</sub>O<sub>4</sub>S [M – H]<sup>–</sup> 365.1, found 365.0.

##### 4.1.6.2. 3-(4-((5-Fluoro-2,4-dioxo-3,4-dihydropyrimidin-1(2H)-yl)methyl)-1H-1,2,3-triazol-1-yl)benzenesulfonamide 10b.

Compound **10b** was obtained according the general procedure earlier

reported using 5-fluoro-1-(prop-2-yn-1-yl)pyrimidine-2,4(1H,3H)-dione **7** (0.1 g, 1.0 eq), 3-azidobenzenesulfonamide **9b** (1.1 eq), CuSO<sub>4</sub> (0.1 eq) and Na ascorbate (0.5 eq) in H<sub>2</sub>O/tBuOH 1/1 (8 ml), 67% yield; m.p. 255–257 °C; silica gel TLC *R<sub>f</sub>* 0.24 (MeOH/CH<sub>2</sub>Cl<sub>2</sub> 10% v/v); δ<sub>H</sub> (400 MHz, DMSO-*d*<sub>6</sub>): 11.93 (s, 1H, exchange with D<sub>2</sub>O, CONHCO), 8.94 (s, 1H, Ar-H), 8.39 (s, 1H, Ar-H), 8.27 (d, *J* = 6.6 Hz, 1H, Ar-H), 8.16 (d, *J* = 7.5 Hz, 1H, Ar-H), 7.96 (d, *J* = 7.3 Hz, 1H, Ar-H), 7.84 (t, *J* = 7.9 Hz, 1H, Ar-H), 7.62 (s, 2H, exchange with D<sub>2</sub>O, SO<sub>2</sub>NH<sub>2</sub>), 5.06 (s, 2H, CH<sub>2</sub>); δ<sub>C</sub> (100 MHz, DMSO-*d*<sub>6</sub>): 158.55 (d, *J*<sub>CF</sub> = 38.3 Hz), 150.55, 146.85, 145.02, 140.86 (d, *J*<sub>CF</sub> = 224.8 Hz), 137.70, 131.98, 130.95 (d, *J*<sub>CF</sub> = 45.9 Hz), 126.65, 124.15, 123.11, 118.23, 43.85; δ<sub>F</sub> (376 MHz, DMSO-*d*<sub>6</sub>): 168.95; *m/z* (ESI negative) calcd for C<sub>13</sub>H<sub>10</sub>FN<sub>6</sub>O<sub>4</sub>S [M - H]<sup>-</sup> 365.1, found 365.0.

4.1.6.3. 3-Chloro-4-(4-((5-fluoro-2,4-dioxo-3,4-dihydropyrimidin-1(2H)-yl)methyl)-1H-1,2,3-triazol-1-yl)benzenesulfonamide **10c**. Compound **10c** was obtained according the general procedure earlier reported using 5-fluoro-1-(prop-2-yn-1-yl)pyrimidine-2,4(1H,3H)-dione **7** (0.1 g, 1.0 eq), 4-azido-3-chlorobenzenesulfonamide **9c** (1.1 eq), CuSO<sub>4</sub> (0.1 eq) and Na ascorbate (0.5 eq) in H<sub>2</sub>O/tBuOH 1/1 (8 ml). 48% yield; m.p. 276–278 °C; silica gel TLC *R<sub>f</sub>* 0.30 (MeOH/CH<sub>2</sub>Cl<sub>2</sub> 10% v/v); δ<sub>H</sub> (400 MHz, DMSO-*d*<sub>6</sub>): 11.91 (s, 1H, exchange with D<sub>2</sub>O, CONHCO), 8.70 (s, 1H, Ar-H), 8.29 (s, 1H, Ar-H), 8.17 (d, *J* = 1.7 Hz, 1H, Ar-H), 8.01 (dd, *J* = 8.3, 1.8 Hz, 1H, Ar-H), 7.96 (d, *J* = 8.3 Hz, 1H, Ar-H), 7.76 (s, 2H, exchange with D<sub>2</sub>O, SO<sub>2</sub>NH<sub>2</sub>), 5.08 (s, 2H, CH<sub>2</sub>); δ<sub>C</sub> (100 MHz, DMSO-*d*<sub>6</sub>): 158.52 (d, *J*<sub>CF</sub> = 37.0 Hz), 150.51, 147.61, 143.75, 140.96 (d, *J*<sub>CF</sub> = 233.5 Hz), 137.73, 130.99 (d, *J*<sub>CF</sub> = 33.9 Hz), 130.22, 129.97, 128.76, 126.86, 126.66, 43.66; δ<sub>F</sub> (376 MHz, DMSO-*d*<sub>6</sub>): 169.03; *m/z* (ESI negative) calcd for C<sub>13</sub>H<sub>9</sub>ClFN<sub>6</sub>O<sub>4</sub>S [M - H]<sup>-</sup> 399.0, found 399.1.

4.1.6.4. 3-Bromo-4-(4-((5-fluoro-2,4-dioxo-3,4-dihydropyrimidin-1(2H)-yl)methyl)-1H-1,2,3-triazol-1-yl)benzenesulfonamide **10d**. Compound **10d** was obtained according the general procedure earlier reported using 5-fluoro-1-(prop-2-yn-1-yl)pyrimidine-2,4(1H,3H)-dione **7** (0.1 g, 1.0 eq), 4-azido-3-bromobenzenesulfonamide **9d** (1.1 eq), CuSO<sub>4</sub> (0.1 eq) and Na ascorbate (0.5 eq) in H<sub>2</sub>O/tBuOH 1/1 (8 ml). 45% yield; m.p. 275–277 °C; silica gel TLC *R<sub>f</sub>* 0.28 (MeOH/CH<sub>2</sub>Cl<sub>2</sub> 10% v/v); δ<sub>H</sub> (400 MHz, DMSO-*d*<sub>6</sub>): 11.91 (s, 1H, exchange with D<sub>2</sub>O, CONHCO), 8.67 (s, 1H, Ar-H), 8.30 (s, 2H, Ar-H), 8.03 (d, *J* = 7.9 Hz, 1H, Ar-H), 7.90 (d, *J* = 8.2 Hz, 1H, Ar-H), 7.75 (s, 2H, exchange with D<sub>2</sub>O, SO<sub>2</sub>NH<sub>2</sub>), 5.08 (s, 2H, CH<sub>2</sub>); δ<sub>C</sub> (100 MHz, DMSO-*d*<sub>6</sub>): 158.58 (d, *J*<sub>CF</sub> = 31.9 Hz), 150.49, 147.79, 143.65, 140.83 (d, *J*<sub>CF</sub> = 230.1 Hz), 139.47, 131.73, 130.95 (d, *J*<sub>CF</sub> = 37.0 Hz), 130.48, 127.10, 126.83, 120.16, 43.63; δ<sub>F</sub> (376 MHz, DMSO-*d*<sub>6</sub>): 169.02; *m/z* (ESI negative) calcd for C<sub>13</sub>H<sub>9</sub>BrFN<sub>6</sub>O<sub>4</sub>S [M - H]<sup>-</sup> 443.0, found 442.9.

#### 4.1.7. 5-Fluoro-1-((1-(4-methyl-2-oxo-2H-chromen-7-yl)-1H-1,2,3-triazol-4-yl)methyl)pyrimidine-2,4(1H,3H)-dione **14**

Compound **14** was obtained according the general procedure earlier reported using 5-fluoro-1-(prop-2-yn-1-yl)pyrimidine-2,4(1H,3H)-dione **7** (0.1 g, 1.0 eq), 7-azido-4-methyl-chromen-2-one **13** (1.1 eq), CuSO<sub>4</sub> (0.1 eq) and Na ascorbate (0.5 eq) in H<sub>2</sub>O/tBuOH 1/1 (8 ml). 47% yield; m.p. 282–284 °C; silica gel TLC *R<sub>f</sub>* 0.30 (MeOH/CH<sub>2</sub>Cl<sub>2</sub> 10% v/v); δ<sub>H</sub> (400 MHz, DMSO-*d*<sub>6</sub>): 11.93 (s, 1H, exchange with D<sub>2</sub>O, CONHCO), 9.00 (s, 1H, Ar-H), 8.28 (d, *J* = 6.5 Hz, 1H, Ar-H), 8.00 (d, *J* = 9.3 Hz, 3H, Ar-H), 6.51 (s, 1H, Ar-H), 5.03 (s, 2H, CH<sub>2</sub>), 2.51 (s, 3H, CH<sub>3</sub>); δ<sub>C</sub> (100 MHz, DMSO-*d*<sub>6</sub>): 160.43, 158.71 (d, *J*<sub>CF</sub> = 22.7 Hz), 154.68, 153.74, 150.53, 143.65 (d, *J*<sub>CF</sub> = 311.3 Hz), 139.80, 139.44, 130.99 (d, *J*<sub>CF</sub> = 42.8 Hz), 128.27, 122.96, 120.56, 116.45, 115.7, 108.45, 43.87, 19.15; δ<sub>F</sub> (376 MHz, DMSO-*d*<sub>6</sub>): 168.91; *m/z* (ESI negative) calcd for C<sub>17</sub>H<sub>11</sub>FN<sub>5</sub>O<sub>4</sub> [M - H]<sup>-</sup> 368.1 found 368.0.

#### 4.1.8. Synthesis of 2-(5-fluoro-2,4-dioxo-3,4-dihydropyrimidin-1(2H)-yl)-N-(4-methyl-2-oxo-2H-chromen-7-yl)acetamide **12a**

EDCI (2.0 eq) was added to a solution of 1-carboxymethyl 5-fluorouracil **2** (0.2 g, 1.0 eq) and HOBt (0.5 eq) in dry DMF (2 ml) under a nitrogen atmosphere and the reaction mixture was stirred at r.t. until the consumption of the starting material (TLC monitoring). Thereafter 7-amino-4-methylcoumarin **11a** (1.5 eq) was added to the reaction mixture, that was stirred at r.t. until the disappearance of the activated ester was observed (TLC monitoring) and then quenched with ice and HCl<sub>(aq)</sub> 2M. The collected, water washed precipitate was triturated in MeOH to afford the pure titled compound as a powder. 24% yield; m.p. 274–276 °C; silica gel TLC *R<sub>f</sub>* 0.33 (MeOH/CH<sub>2</sub>Cl<sub>2</sub> 10% v/v); δ<sub>H</sub> (400 MHz, DMSO-*d*<sub>6</sub>): 11.97 (s, 1H, exchange with D<sub>2</sub>O, CONHCO), 10.76 (s, 1H, exchange with D<sub>2</sub>O, CONH), 8.17 (s, 1H, Ar-H), 7.78 (s, 1H, Ar-H), 7.72 (d, *J* = 1.9 Hz, 1H, Ar-H), 7.53 (dd, *J* = 8.7, 2.0 Hz, 1H, Ar-H), 6.32 (d, *J* = 1.0 Hz, 1H, Ar-H), 4.59 (s, 2H, CH<sub>2</sub>), 2.44 (s, 3H, CH<sub>3</sub>); δ<sub>C</sub> (100 MHz, DMSO-*d*<sub>6</sub>): 167.21, 160.99, 158.58 (d, *J*<sub>CF</sub> = 25.8 Hz), 154.73, 154.11, 150.87, 142.78, 140.38 (d, *J*<sub>CF</sub> = 228.7 Hz), 132.07 (d, *J*<sub>CF</sub> = 33.8 Hz), 127.23, 116.43, 116.19, 113.59, 106.76, 51.43, 19.03; δ<sub>F</sub> (376 MHz, DMSO-*d*<sub>6</sub>): 170.35; *m/z* (ESI negative) calcd for C<sub>16</sub>H<sub>11</sub>FN<sub>3</sub>O<sub>5</sub> [M - H]<sup>-</sup> 344.1, found 344.0.

#### 4.1.9. Synthesis of 2-oxo-2H-chromen-7-yl 2-(5-fluoro-2,4-dioxo-3,4-dihydropyrimidin-1(2H)-yl)acetate **12b**

EDCI (2.0 eq) was added to a solution of 1-carboxymethyl 5-fluorouracil **2** (0.2 g, 1.0 eq) and DMAP (0.03 eq) in dry DMF (2 ml) under a nitrogen atmosphere and the reaction mixture was stirred at r.t. until the consumption of the starting material (TLC monitoring). Thereafter 7-hydroxycoumarin **11b** (1.5 eq) was added to the reaction mixture, that was stirred at r.t. until the disappearance of the 1-carboxymethyl 5-fluorouracil was observed (TLC monitoring) and then quenched with ice and sodium bicarbonate. The collected, water-washed precipitate triturated with ethylacetate to afford the pure titled compound **12b** as a powder. 15% yield; m.p. 270–272 °C; silica gel TLC *R<sub>f</sub>* 0.45 (MeOH/CH<sub>2</sub>Cl<sub>2</sub> 20% v/v); δ<sub>H</sub> (400 MHz, DMSO-*d*<sub>6</sub>): 12.08 (s, 1H, exchange with D<sub>2</sub>O, CONHCO), 8.17 (d, *J* = 6.7 Hz, 1H, Ar-H), 8.09 (d, *J* = 9.6 Hz, 1H, Ar-H), 7.80 (dd, *J* = 17.8, 8.5 Hz, 1H, Ar-H), 7.30 (s, 1H, Ar-H), 7.21 (dd, *J* = 8.5, 2.2 Hz, 1H, Ar-H), 6.51 (d, *J* = 9.6 Hz, 1H, Ar-H), 4.78 (d, *J* = 32.0 Hz, 2H, CH<sub>2</sub>); δ<sub>C</sub> (100 MHz, DMSO-*d*<sub>6</sub>): 167.62, 160.66, 158.47 (d, *J*<sub>CF</sub> = 25.8 Hz), 155.16, 153.26, 150.77, 144.80, 140.57 (d, *J*<sub>CF</sub> = 230.2 Hz), 131.21 (d, *J*<sub>CF</sub> = 34.7 Hz), 130.69, 119.25, 118.16, 116.95, 110.76, 49.85; δ<sub>F</sub> (376 MHz, DMSO-*d*<sub>6</sub>): 169.21; *m/z* (ESI negative) calcd for C<sub>15</sub>H<sub>8</sub>FN<sub>2</sub>O<sub>6</sub> [M - H]<sup>-</sup> 331.0, found 331.0.

## 4.2. Carbonic anhydrases inhibition

An Applied Photophysics stopped-flow instrument has been used for assaying the CA catalysed CO<sub>2</sub> hydration activity [22]. Phenol red (at a concentration of 0.2 mM) has been used as indicator, working at the absorbance maximum of 557 nm, with 20 mM Hepes (pH 7.5) as buffer, and 20 mM Na<sub>2</sub>SO<sub>4</sub> (for maintaining constant the ionic strength), following the initial rates of the CA-catalysed CO<sub>2</sub> hydration reaction for a period of 10–100 s. The CO<sub>2</sub> concentrations ranged from 1.7 to 17 mM for the determination of the kinetic parameters and inhibition constants. For each inhibitor at least six traces of the initial 5–10% of the reaction have been used for determining the initial velocity. The uncatalyzed rates were determined in the same manner and subtracted from the total observed rates. Stock solutions of inhibitor (0.1 mM) were prepared in distilled-deionized water and dilutions up to 0.01 nM were done thereafter with the assay buffer. Inhibitor and enzyme solutions were preincubated together for 15 min (sulfonamides) or 6 h (coumarins) at room temperature prior to assay, in order to

allow for the formation of the E-I complex. The inhibition constants were obtained by non-linear least-squares methods using PRISM 3 and the Cheng-Prusoff equation, as reported earlier [23,24], and represent the mean from at least three different determinations. All CA isoforms were recombinant ones obtained in-house as reported earlier [25].

#### 4.3. X-ray crystallography

CA II was expressed and purified as previously described [26]. In brief, CA II was expressed in BL21(DE3) *E. coli* cells and induced with IPTG. Protein was purified from lysed cells using affinity chromatography with p-(aminomethyl)benzenesulfonamide resin. Final protein purity was confirmed via SDS-PAGE and the purified CA II diluted to a final concentration of 10 mg/mL for crystallization. Complex formation was induced by co-crystallization using the hanging drop vaporization method in which CA II crystals were grown in the presence of 350  $\mu$ M compound **A**. A precipitant solution of 1.6 M NaCitrate, 50 mM Tris, pH 7.8 was used and crystal formation observed within 3–5 days. Crystals were transferred into a cryoprotectant of 20% glycerol before flash cooling in liquid nitrogen for shipment to the synchrotron.

Diffraction data was collected on the F1 beamline at Cornell High Energy Synchrotron Source (CHESS) using a Pilatus 6M detector. Data sets were collected with a crystal-to-detector distance of 260 mm, 1° oscillation angle, and exposure time of 1 s for a total of 180 images. The data was indexed and integrated in XDS [27] and then scaled to the P<sub>2</sub> space group using Aimless [28]. Phases were determined by molecular replacement using a search model of CA II (PDB: 3KS3 [29]) followed by structure refinements in Phenix [30] (Table 4). Finally, Coot [31] was used to analyze inhibitor interactions and PyMol [32] for figure production.

#### 4.4. Anticancer activity

##### 4.4.1. In vitro anti-proliferative activity

The eight examined cancer cell lines (Hela, Colo-205, A-549, HL-60, SKOV-3, MDA-MB-231, MCF-7 and T47D) were obtained from American Type Culture Collection (ATCC). The cells were grown in RPMI or DMEM media supplemented with 100 mg/mL of streptomycin, 100 units/mL of penicillin and 10% of heat-inactivated fetal bovine serum in humidified, 5% (v/v) CO<sub>2</sub> atmosphere at 37 °C. Cytotoxicity was assessed by the use of the SRB colorimetric assay [33], as described earlier [34].

##### 4.4.2. Cell cycle analysis

Cell cycle distributions in breast cancer T-47D cells were examined by the use of PI staining and analyzed via flow cytometry using FACS Calibur upon treatment with sulfonamides **4e** and **6d** at their IC<sub>50</sub> concentration (7.56 and 2.45  $\mu$ M, respectively), as described previously [35,36]. The cell cycle distributions were calculated using CellQuest software (Becton Dickinson).

##### 4.4.3. Annexin V-FITC apoptosis assay

Phosphatidylserine externalization impact of sulfonamides **4e** and **6d** towards breast cancer T-47D cell line was examined using FITC Annexin-V Apoptosis Detection Kit by flow cytometry, following the manufacturer's protocol and referring to the reported procedures [35].

#### Declaration of competing interest

The authors declare that they have no known competing financial interests or personal relationships that could have appeared to influence the work reported in this paper.

#### Acknowledgements

MIUR is gratefully acknowledged for a grant to A.N (PRIN: rot. 2017XYBP2R). This work was in part funded by the Researchers Supporting Project No. (RSP-2019/1) King Saud University, Riyadh, Saudi Arabia.

#### Appendix A. Supplementary data

Supplementary data to this article can be found online at <https://doi.org/10.1016/j.ejmech.2020.112112>.

#### Associated content

The atomic coordinates of the CA II/A complex have been deposited in the Protein Data Bank with accession code 6VJ3.

#### References

- [1] M.L. Taddei, E. Giannoni, G. Comito, P. Chiarugi, Microenvironment and tumor cell plasticity: an easy way out, *Canc. Lett.* 341 (2013) 80–96.
- [2] E.C. Finger, A.J. Giaccia, Hypoxia, inflammation, and the tumor microenvironment in metastatic disease, *Canc. Metastasis Rev.* 29 (2010) 285–293.
- [3] D. Neri, C.T. Supuran, Interfering with pH regulation in tumours as a therapeutic strategy, *Nat. Rev. Drug Discov.* 10 (2011) 767–777.
- [4] A. Nocentini, C.T. Supuran, Carbonic anhydrase inhibitors as antitumor/anti-metastatic agents: a patent review (2008–2018), *Expert Opin. Ther. Pat.* 28 (2018) 729–740.
- [5] R.A. Gatenby, K. Smallbone, P.K. Maini, F. Rose, J. Averill, R.B. Nagle, L. Worrall, R.J. Gillies, Cellular adaptations to hypoxia and acidosis during somatic evolution of breast cancer, *Br. J. Canc.* 97 (2007) 646–653.
- [6] C.T. Supuran, Carbonic anhydrases: novel therapeutic applications for inhibitors and activators, *Nat. Rev. Drug Discov.* 7 (2008) 168–181.
- [7] A. Nocentini, C.T. Supuran, Carbonic anhydrases: an overview, in: A. Nocentini, C.T. Supuran (Eds.), *Carbonic Anhydrases*, Elsevier, Amsterdam, 2019, pp. 3–16.
- [8] V. Alterio, M. Hilvo, A. Di Fiore, C.T. Supuran, P. Pan, S. Parkkila, A. Scaloni, J. Pastorek, S. Pastorekova, C. Pedone, A. Scozzafava, S.M. Monti, G. De Simone, Crystal structure of the catalytic domain of the tumor-associated human carbonic anhydrase IX, *Proc. Natl. Acad. Sci. U.S.A.* 106 (2009) 16233–16238.
- [9] D.A. Whittington, A. Waheed, B. Ulmasov, G.N. Shah, J.H. Grubb, W.S. Sly, D.W. Christianson, Crystal structure of the dimeric extracellular domain of human carbonic anhydrase XII, a bitopic membrane protein overexpressed in certain cancer tumor cells, *Proc. Natl. Acad. Sci. U.S.A.* 98 (2001) 9545–9550.
- [10] C.T. Supuran, V. Alterio, A. Di Fiore, K. D' Ambrosio, F. Carta, S.M. Monti, G. De Simone, Inhibition of carbonic anhydrase IX targets primary tumors, metastases, and cancer stem cells: three for the price of one, *Med. Res. Rev.* 38 (2018) 1799–1836.
- [11] C.T. Supuran, How many carbonic anhydrase inhibition mechanisms exist, *J. Enzym. Inhib. Med. Chem.* 31 (2016) 345–360.
- [12] A. Nocentini, C.T. Supuran, Advances in the structural annotation of human carbonic anhydrases and impact on future drug discovery, *Expert Opin. Drug Discov.* 14 (2019) 1175–1197.
- [13] C.L. Lomelino, J.T. Andring, R. McKenna, Crystallography and its impact on carbonic anhydrase research, *Int. J. Med. Chem.* 2018 (2018) 9419521.
- [14] <https://clinicaltrials.gov/ct2/show/NCT03450018>. (Accessed 9 January 2020).
- [15] A. Nocentini, S. Bua, C.L. Lomelino, R. McKenna, M. Menicatti, G. Bartolucci, B. Tenci, L. Di Cesare Mannelli, C. Ghelardini, P. Gratteri, C.T. Supuran, Discovery of new sulfonamide carbonic anhydrase IX inhibitors incorporating nitrogenous bases, *ACS Med. Chem. Lett.* 8 (2017) 1314–1319.
- [16] A. Palasz, Ciez Dariusz, In search of uracil derivatives as bio-active agents. Uracils and fused uracils: synthesis, biological activity and applications, *Eur. J. Med. Chem.* 97 (2015) 582–611.
- [17] M. Legraverend, D.S. Grierson, The purines: potent and versatile small molecule inhibitors and modulators of key biological targets, *Bioorg. Med. Chem.* 14 (2006) 3987–4006.
- [18] W.B. Parker, Enzymology of purine and pyrimidine antimetabolites used in the treatment of cancer, *Chem. Rev.* 109 (2009) 2880–2893.
- [19] J. Calderón-Arancibia, C. Espinosa-Bustos, A. Cañete-Molina, R.A. Tapia, M. Faúndez, M.J. Torres, A. Aguirre, M. Paulino, C.O. Salas, Synthesis and pharmacophore modelling of 2,6,9-trisubstituted purine derivatives and their potential role as apoptosis-inducing agents in cancer cell lines, *Molecules* 20 (2015) 6808–6826.
- [20] B. Daniel, D. Longley, Harkin Paul, G. Patrick, Johnston, 5-Fluorouracil: mechanisms of action and clinical strategies, *Nat. Rev. Canc.* 3 (2003) 330–338.
- [21] L.K. Gediya, V.C. Njar, Promise and challenges in drug discovery and development of hybrid anticancer drugs, *Expert Opin. Drug Discov.* 4 (2009) 1099–1111.

- [22] R.G. Khalifah, The carbon dioxide hydration activity of carbonic anhydrase, *J. Biol. Chem.* 246 (1971) 2561–2573.
- [23] A. Nocentini, M. Ceruso, S. Bua, C.L. Lomelino, J.T. Andring, R. McKenna, C. Lanzi, S. Sgambellone, R. Pecori, R. Matucci, L. Filippi, P. Gratteri, F. Carta, E. Masini, S. Selleri, C.T. Supuran, Discovery of  $\beta$ -adrenergic receptors blocker-carbonic anhydrase inhibitor hybrids for multitargeted antiglaucoma therapy, *J. Med. Chem.* 61 (2018) 5380–5394.
- [24] A. Nocentini, P. Gratteri, C.T. Supuran, Phosphorus versus sulfur: discovery of benzenephosphonamidates as versatile sulfonamide-mimic chemotypes acting as carbonic anhydrase inhibitors, *Chem. Eur. J.* 25 (2019) 1188–1192.
- [25] A. Nocentini, E. Trallori, S. Singh, C.L. Lomelino, G. Bartolucci, L. Di Cesare Mannelli, C. Ghelardini, R. McKenna, P. Gratteri, C.T. Supuran, 4-Hydroxy-3-nitro-5-ureido-benzenesulfonamides selectively target the tumor-associated carbonic anhydrase isoforms IX and XII showing hypoxia-enhanced anti-proliferative profiles, *J. Med. Chem.* 61 (2018) 10860–10874.
- [26] M.A. Pinard, C.D. Boone, B.D. Rife, C.T. Supuran, R. McKenna, Structural study of interaction between brinzolamide and dorzolamide inhibition of human carbonic anhydrases, *Bioorg. Med. Chem.* 21 (2013) 7210–7215.
- [27] W. Kabsch, XDS, *Acta Crystallogr. D* 66 (2010) 125–132.
- [28] M.D. Winn, C.C. Ballard, K.D. Cowtan, E.J. Dodson, P. Emsley, P.R. Evans, R.M. Keegan, E.B. Krissinel, A.G. Leslie, A. McCoy, S.J. McNicholas, G.N. Murshudov, N.S. Pannu, E.A. Potterton, H.R. Powell, R.J. Read, A. Vagin, K.S. Wilson, Overview of the CCP4 suite and current developments, *Acta Crystallogr. D* 67 (2011) 235–242.
- [29] B.S. Avvaru, C.U. Kim, H. Katherine, M. Sol, N. David, R. McKenna, A short, strong hydrogen bond in the active site of human carbonic anhydrase II, *Biochemistry (Mosc.)* 49 (2010) 249–251.
- [30] P.D. Adams, V. Afonine, G. Bunkóczi, V.B. Chen, I.W. Davis, N. Echols, J.J. Headd, L.W. Hung, G.J. Kapral, R.W. Grosse-Kunstleve, A.J. McCoy, N.W. Moriarty, R. Oeffner, R.J. Read, D.C. Richardson, J.S. Richardson, T.C. Terwilliger, P.H. Zwart, PHENIX: a comprehensive Python-based system for macromolecular structure solution, *Acta Crystallogr. Sect. D Biol. Crystallogr.* 66 (2010) 213–221.
- [31] P. Emsley, K. Cowtan, Coot: model-building tools for molecular graphics, *Acta Crystallogr. Sect. D Biol. Crystallogr.* 60 (2004) 2126–2132.
- [32] The PyMOL Molecular Graphics System, Version 1.5.0.4 Schrödinger, LLC.
- [33] P. Skehan, R. Storeng, D. Scudiero, A. Monks, J. McMahon, D. Vistica, J.T. Warren, H. Bokesch, S. Kenney, M.R. Boyd, New colorimetric cytotoxicity assay for anticancer-drug screening, *J. Natl. Cancer Inst.* 82 (1990) 1107–1112.
- [34] W.M. Eldehna, A.M. El Kerdawy, G.H. Al-Ansary, S.T. Al-Rashood, M.M. Ali, Abeer E. Mahmoud, Type IIA-Type IIB protein tyrosine kinase inhibitors hybridization as an efficient approach for potent multikinase inhibitor development: design, synthesis, anti-proliferative activity, multikinase inhibitory activity and molecular modeling of novel indolinone-based ureides and amides, *Eur. J. Med. Chem.* 163 (2019) 37–53.
- [35] W.M. Eldehna, H. Almahli, G.H. Al-Ansary, H.A. Ghabbour, M.H. Aly, O.E. Ismael, A. Al-Dhfyhan, H.A. Abdel-Aziz, Synthesis and in vitro anti-proliferative activity of some novel isatins conjugated with quinazoline/phthalazine hydrazines against triple-negative breast cancer MDA-MB-231 cells as apoptosis-inducing agents, *J. Enzym. Inhib. Med. Chem.* 32 (2017) 600–613.
- [36] W.M. Eldehna, G.S. Hassan, S.T. Al-Rashood, T. Al-Warhi, A.E. Altyar, H.M. Alkahtani, A.A. Almehizia, H.A. Abdel-Aziz, Synthesis and in vitro anti-cancer activity of certain novel 1-(2-methyl-6-arylpyridin-3-yl)-3-phenylureas as apoptosis-inducing agents, *J. Enzym. Inhib. Med. Chem.* 34 (2019) 322–332.